



PHYSICS OF CONFORMAL RADIOTHERAPY

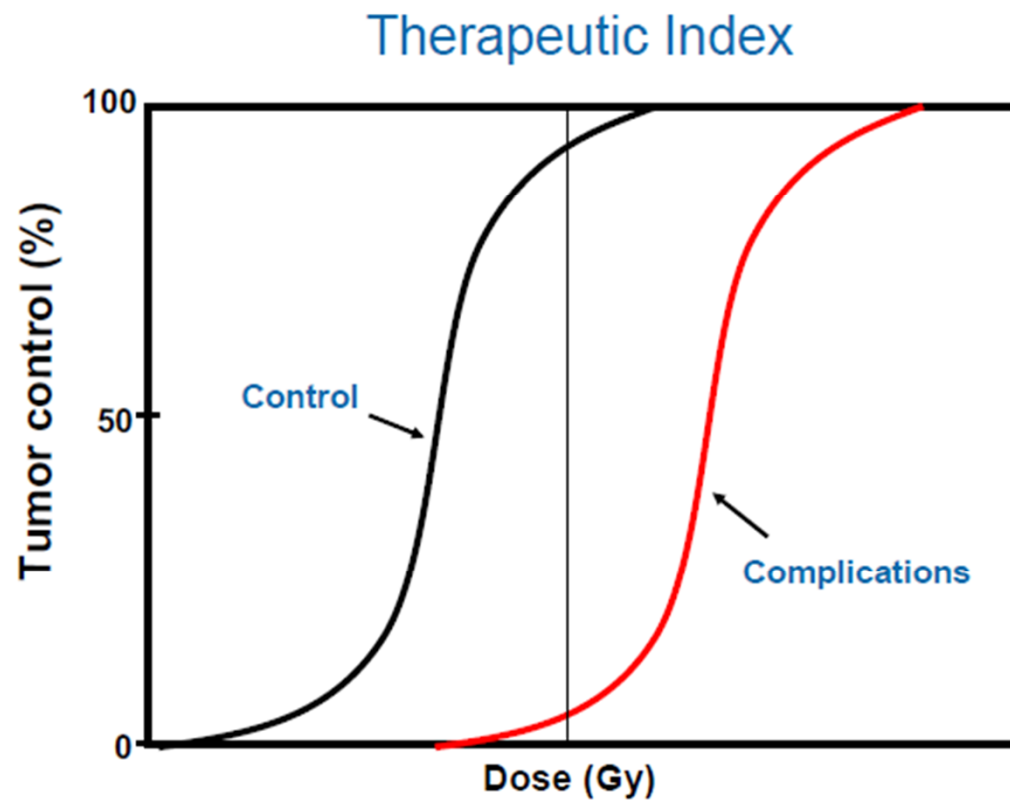
Dr Arabinda Kumar Rath

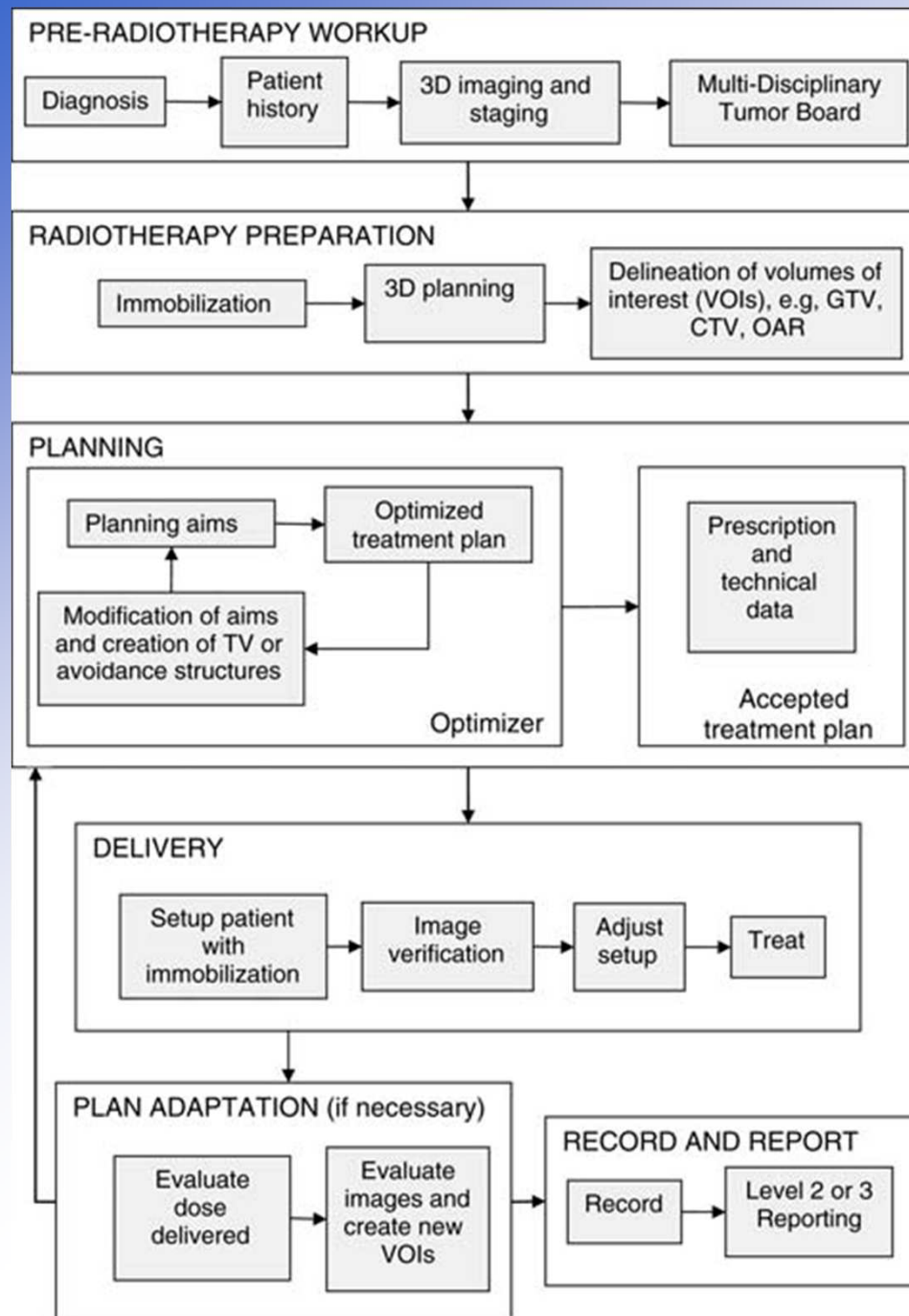
Chairman and MD

Hemalata Hospitals and Research Centre

Bhubaneswar

PRINCIPLE OF RADIOTHERAPY





flow chart of a typical course of radiotherapy

HISTORICAL BACKGROUND



- 2D RT
- 3D Conformal RT
- IMRT
- IGRT
- Adaptive RT
- 4D RT
- SRS/SBRT

ADVANCES IN IMAGING

- Staging
- Patient Selection
- Target volume
 - Less inter-observer variability in contours
- Newer techniques
 - MRI,CT
 - Functional PET – CT/MRI
 - Co-registration software

Immobilisation Techniques

Thermoplastics



- Thermoplastics are long polymers with few cross links.
- They also possess a “plastic memory” - tendency to revert to normal flat shape when reheated

Positioning aids...



Pituitary Board

Prone Support

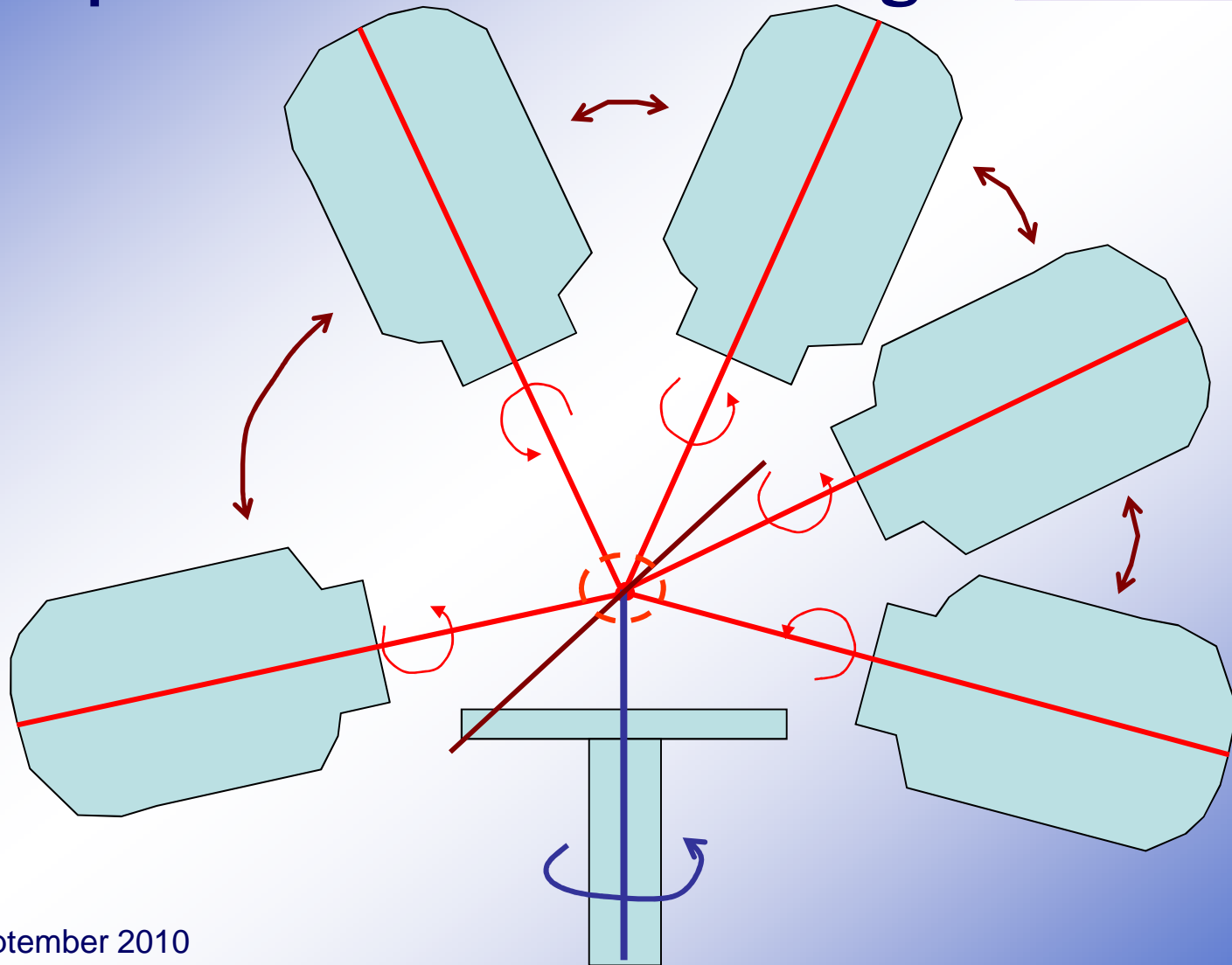


3 way support

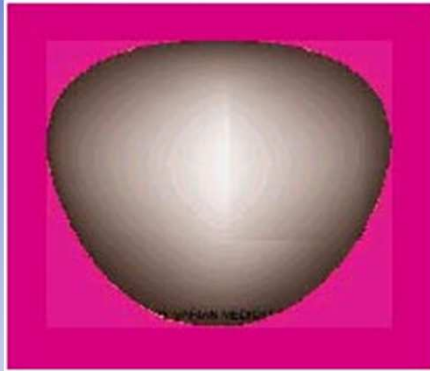


Rotational Radiotherapy

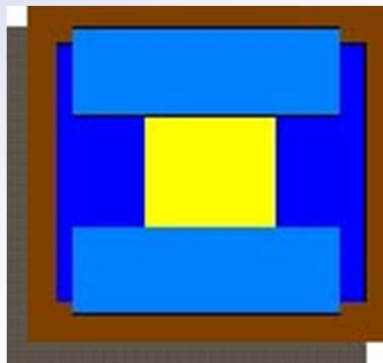
Principle of Isocentric mounting



Conventional Radiotherapy - 1960s



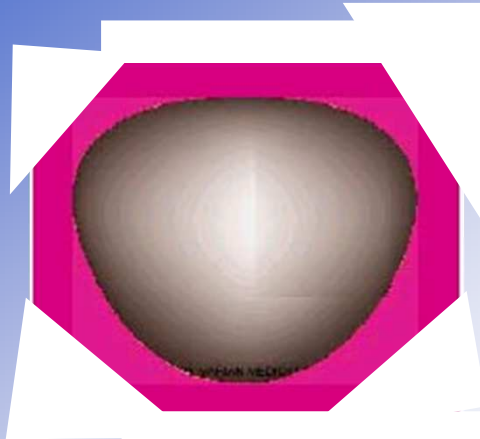
**Pink = treatment field
or area hit by beam**



**Primary collimator
shapes beam**

- Simple treatment delivers uniform dose from 2-4 beam angles
- Beam shape is rectangular or square
- Beam hits healthy tissue as well as tumor
- Doses have to be kept low to minimize harm to normal tissue

Early Beam Shaping - 1970s



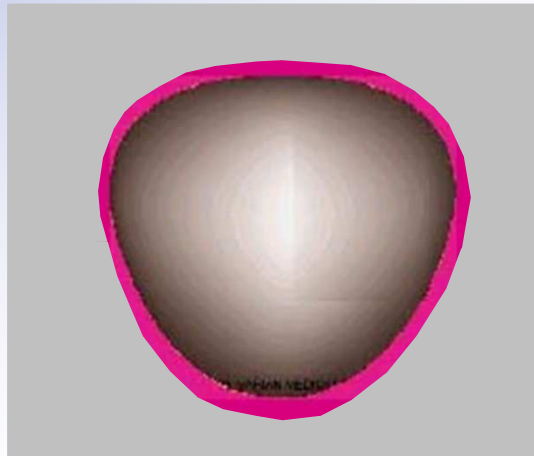
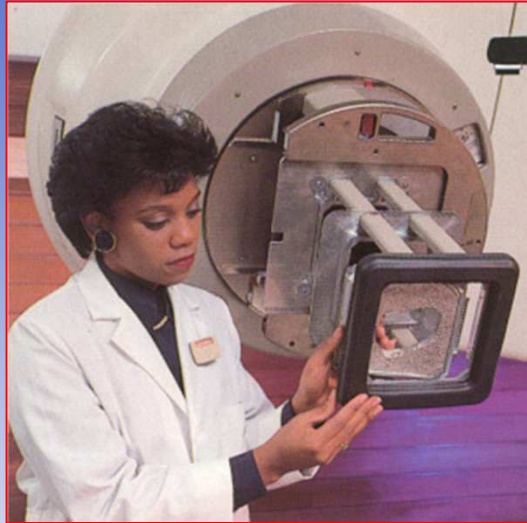
**Roughly shaped
treatment field**



**Wedge helps
shape beam**

- Blocks and wedges used to shape beams and begin sparing healthy tissue
- Blocks are changed by hand for each beam angle
- Labor intensive process requires therapist to visit treatment room repeatedly
- Typical treatments use 4 beam angles
- Dose still relatively low

3-D Conformal Radiation Therapy -1980s



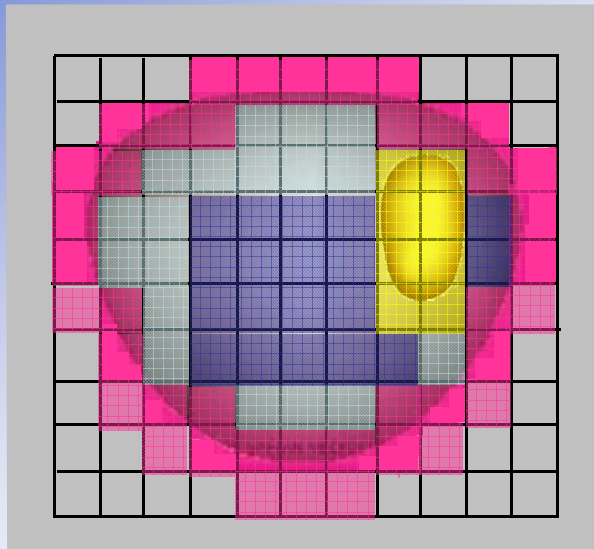
- Custom-molded block(s) match beam shape to tumor profile
- Beam shaping from multiple angles conforms radiation dose to tumor volume
- Typical treatments use 4-6 beam angles
- Dose still relatively low
- Blocks still changed by hand
- Still slow and labor intensive

Intensity Modulated Radiation Therapy (IMRT)



- An advanced form of external beam radiation therapy.
- IMRT offers additional dimension of freedom
 - radiation intensities within a radiation field can be varied within a given beam direction from which the radiation is directed to the tumor.
- This added freedom allows
 - better shape the radiation doses to conform to the target volume while sparing surrounding normal structures.

Intensity Modulated Radiation Therapy (IMRT) - Late 1990s



A Revolution in Radiotherapy

- Divides each treatment field into multiple segments (up to 500/angle)
- ◆ Allows dose escalation to most aggressive tumor cells; best protection of healthy tissue
- ◆ Modulates radiation intensity; gives distinct dose to each segment
- ◆ Uses many beam angles, thousands of segments
- ◆ Improves precision/accuracy
- ◆ Requires inverse treatment planning software to calculate dose distribution

Intensity Modulated Radiation Therapy (IMRT)



- The resulting dosimetric advantage
 - has shown to translate into clinical advantages of improving local and regional tumor control.
- Offers a mechanism for dose escalation
 - to tumors while simultaneously reducing radiation toxicities to the surrounding normal tissue and sensitive structures.
- IMRT combined with stereotactic localization
 - for delivering radiosurgery treatments to intracranial and extracranial sites using linear accelerators

Intensity Modulated Radiation Therapy (IMRT)

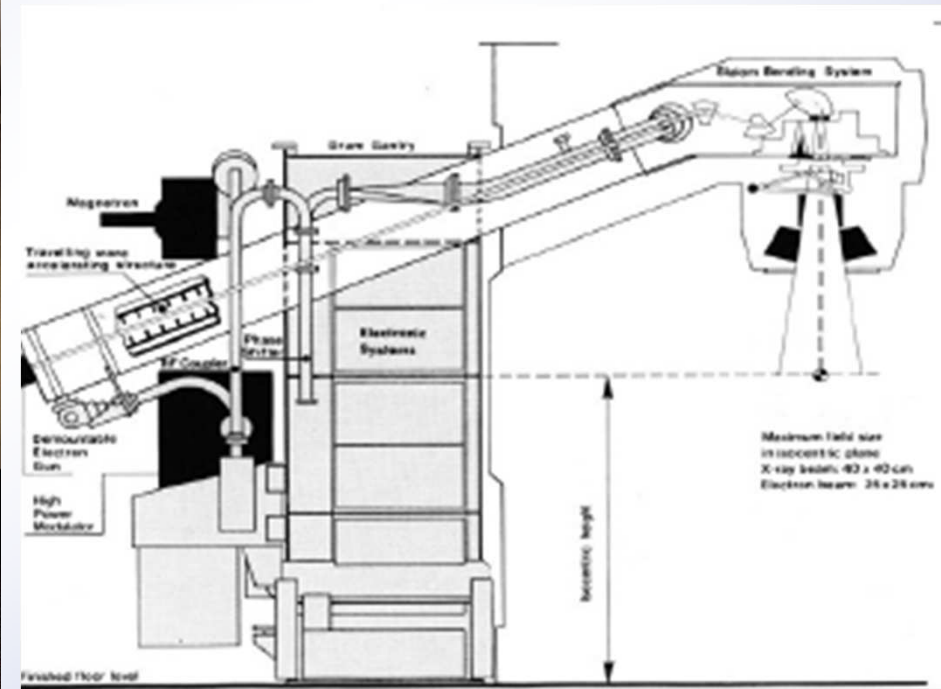


- IMRT spares critical structures
 - by redistributing the normal tissue dose to less critical regions and reducing the high dose volume to just cover the target.
- The reduced toxicity also encouraged the use of hypofractionation schemes.
- The ability of IMRT to
 - paint complex dose distributions
 - allowed concomitant boost
 - the treatment of target within targets

In less than a decade,
Intensity Modulated Radiotherapy
has become common practice in
Radiation Oncology

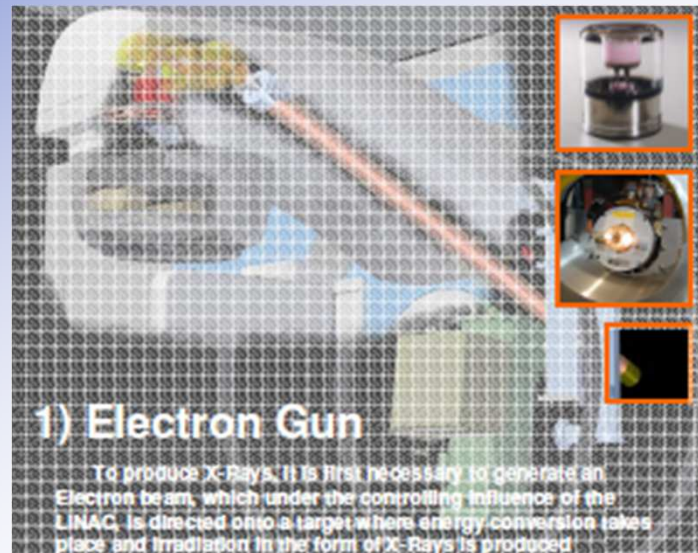
- IMRT technology consists of
 - planning methods and
 - delivery technologies.
- IMRT continues to advance due to improvements in these two areas.

The Medical Linear Accelerator



The Medical Linear Accelerator

Electron Gun



Wave Guide

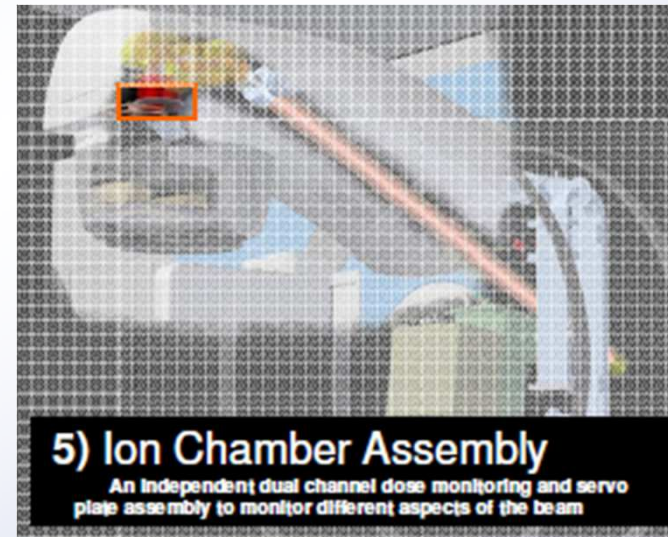


The Medical Linear Accelerator

Bending Magnet

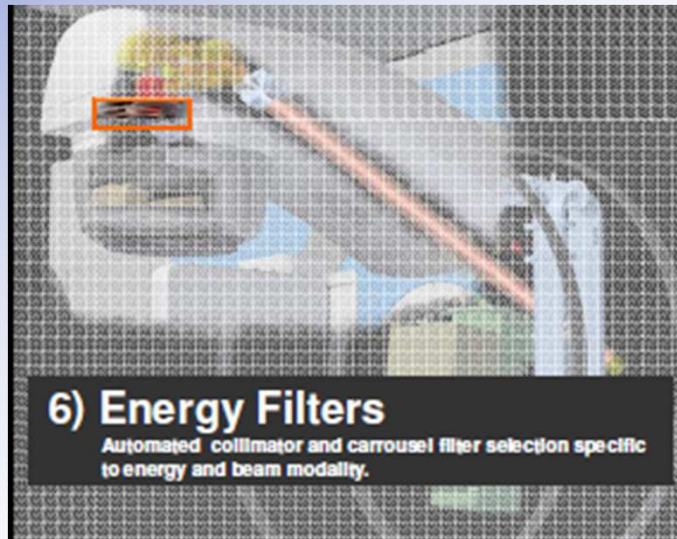


Ion Chamber Assembly



The Medical Linear Accelerator

Energy Filters



X-Rays and Electrons

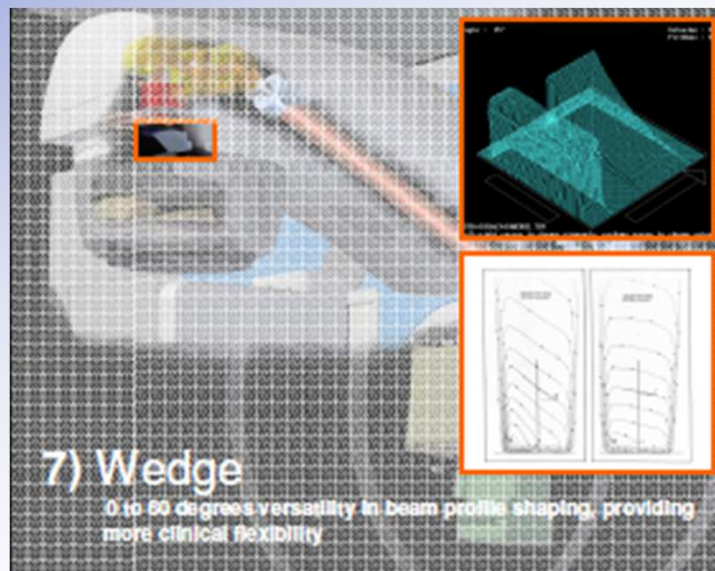
Quick Change Between X-Rays and Electrons

- Automatically selects required flight tube position and filters/foils to satisfy a prescription



The Medical Linear Accelerator

Wedges



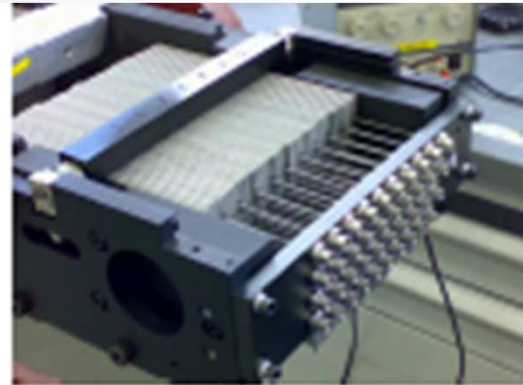
Multi Leaf Collimator



The Medical Linear Accelerator

MLC

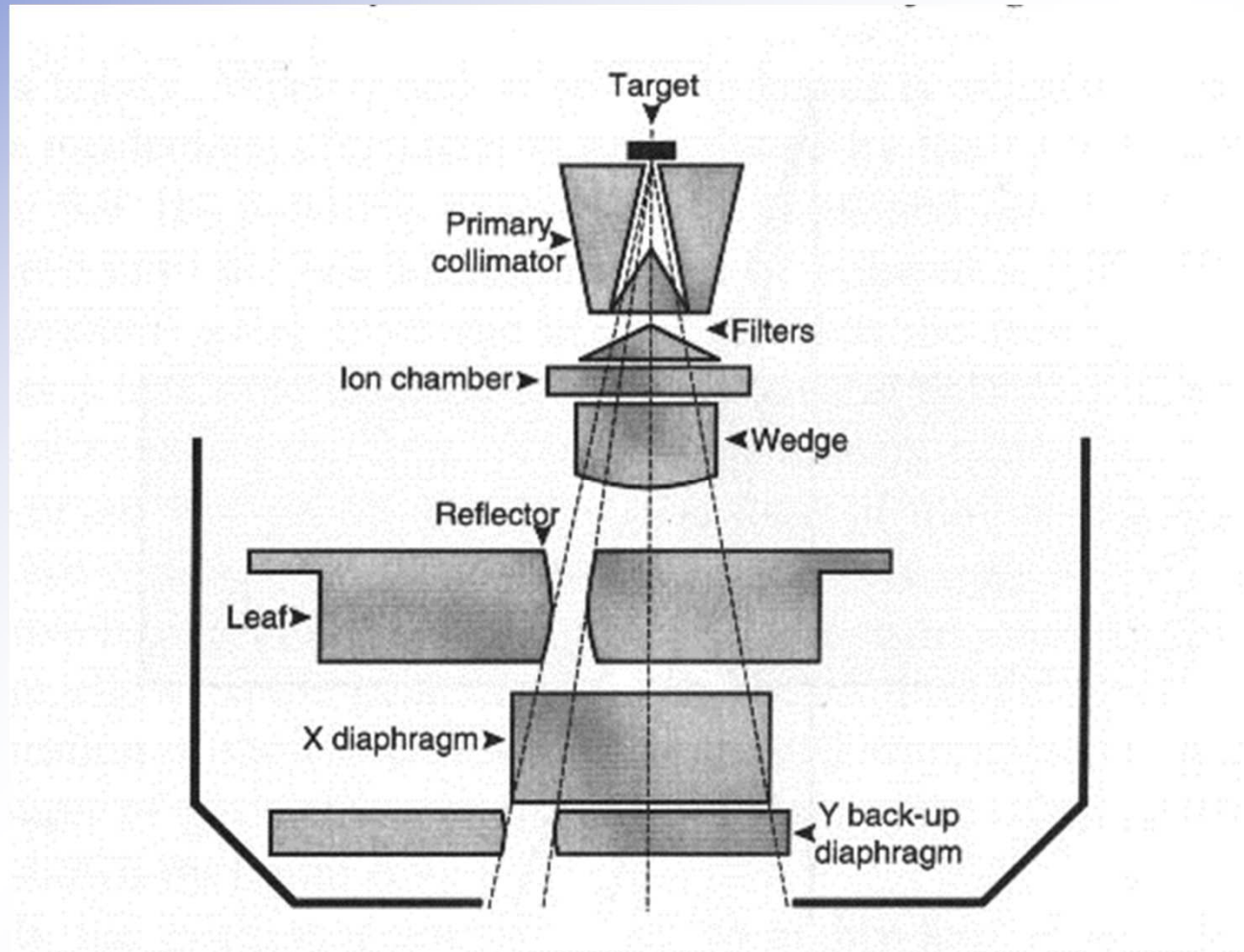
- MLC has bearing guide with lead screw connected to a motor



- Beam modulator has solid leaf guides with rack on leaf and pinion connected to a motor



The Medical Linear Accelerator



Interaction history

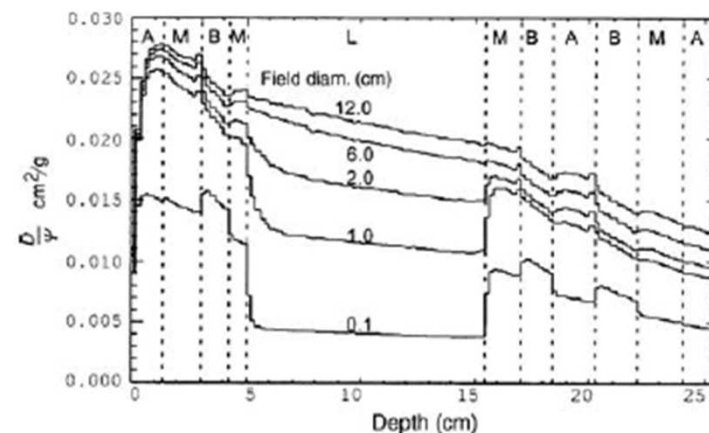
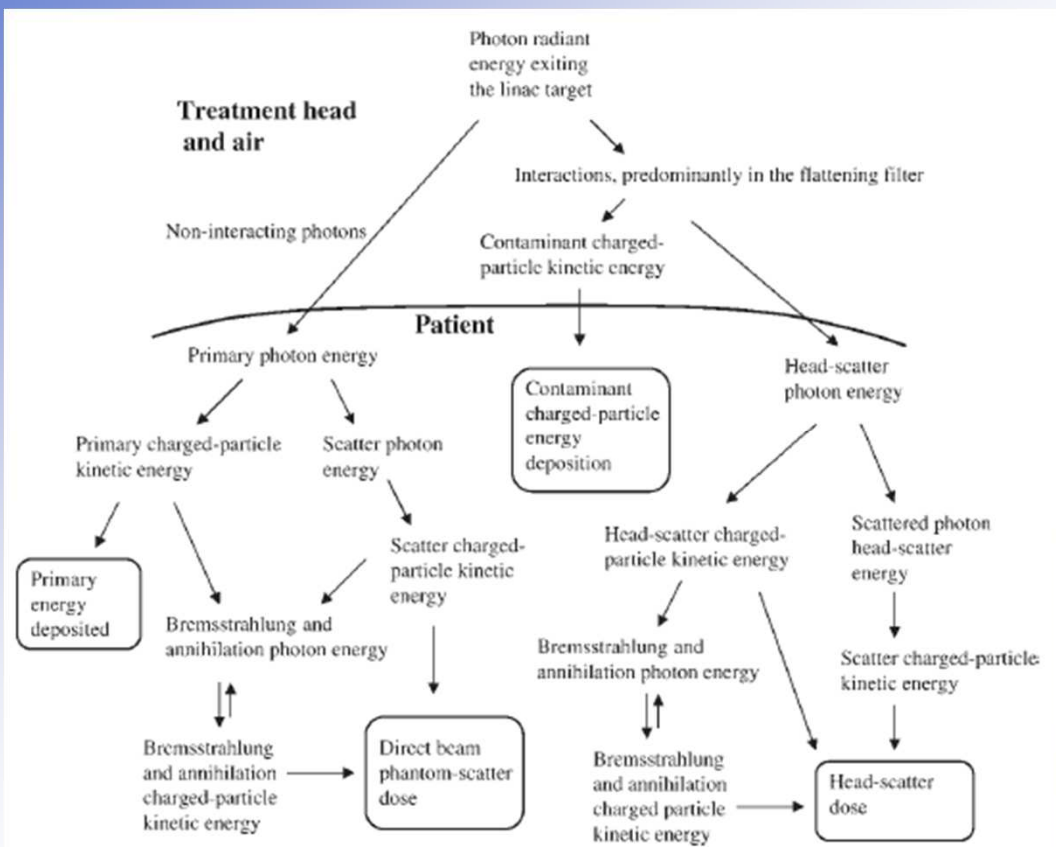
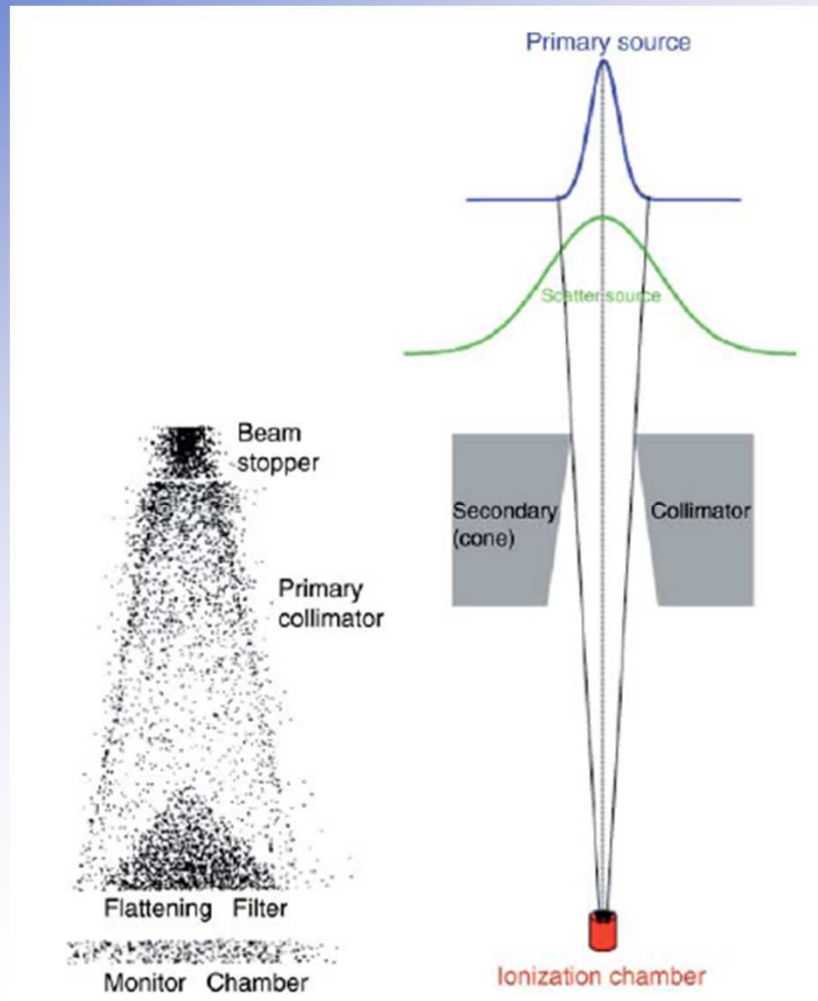


Figure A.1.2. Influence of field size on the depth-dose in a heterogeneous phantom. Shown is absorbed dose per energy fluence along the central axis of a 4 MV parallel beam as a function of depth and beam diameter computed using the convolution/superposition algorithm. The phantom is a slab phantom comprising adipose tissue (A), muscle (M), bone (B), and lung (L). The absorbed-dose reduction in the lung (L), more pronounced at smaller field sizes, is due to the transport of electrons out of the irradiated region in the low-density material. (From Ahnesjö and Aspradakis, 1999; reproduced with permission.)

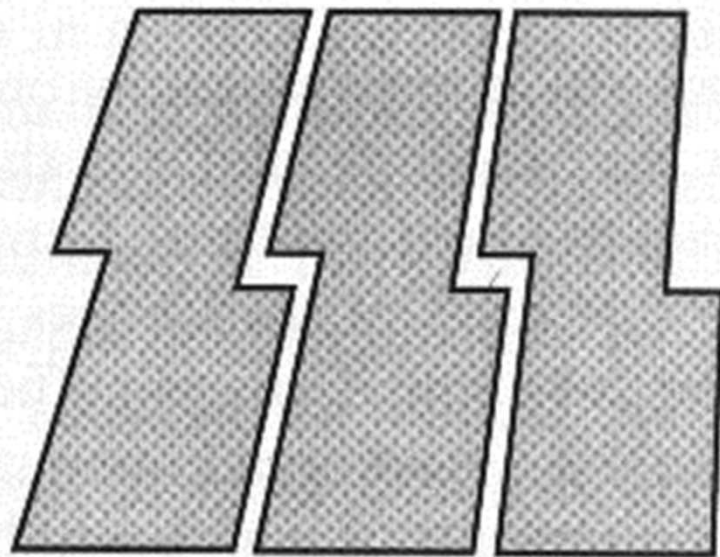
Ahnesjö, A., and Aspradakis, M. M. (1999). "Dose calculations for external photon beams in radiotherapy," *Phys. Med. Biol.* 44, R99–R155.

Beam data modeling

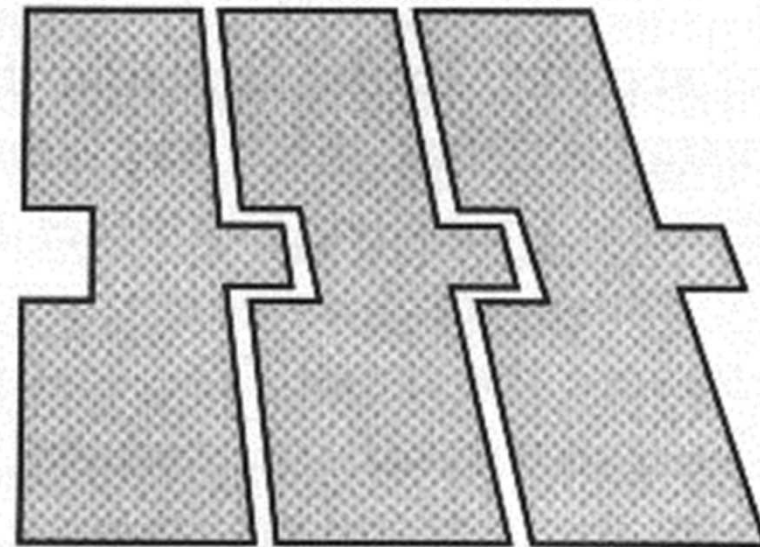


- Left: Scatter plot showing the location of photon scattering events in the treatment head
Chaney, E. L., Cullip, T. J., and Gabriel, T. A. (1994). "A Monte Carlo study of accelerator head scatter," Med. Phys. 21, 1383–1390.
- Right: Dual extended- (non-point-)source model used to describe the fluence at the detector position. The narrow primary-source width is due to the spread of bremsstrahlung production in the target and beam stopper backing the target. The scatter source is indirect (extrafocal) radiation produced mainly by Compton scatter in the field-flattening filter and the primary collimator.
Deng, J., Ma, C.-M., Hai, J., and Nath, R. (2004). "Commissioning 6 MV photon beams of a stereotactic radiosurgery system for Monte Carlo treatment planning," Med. Phys. 30, 3124–3134.

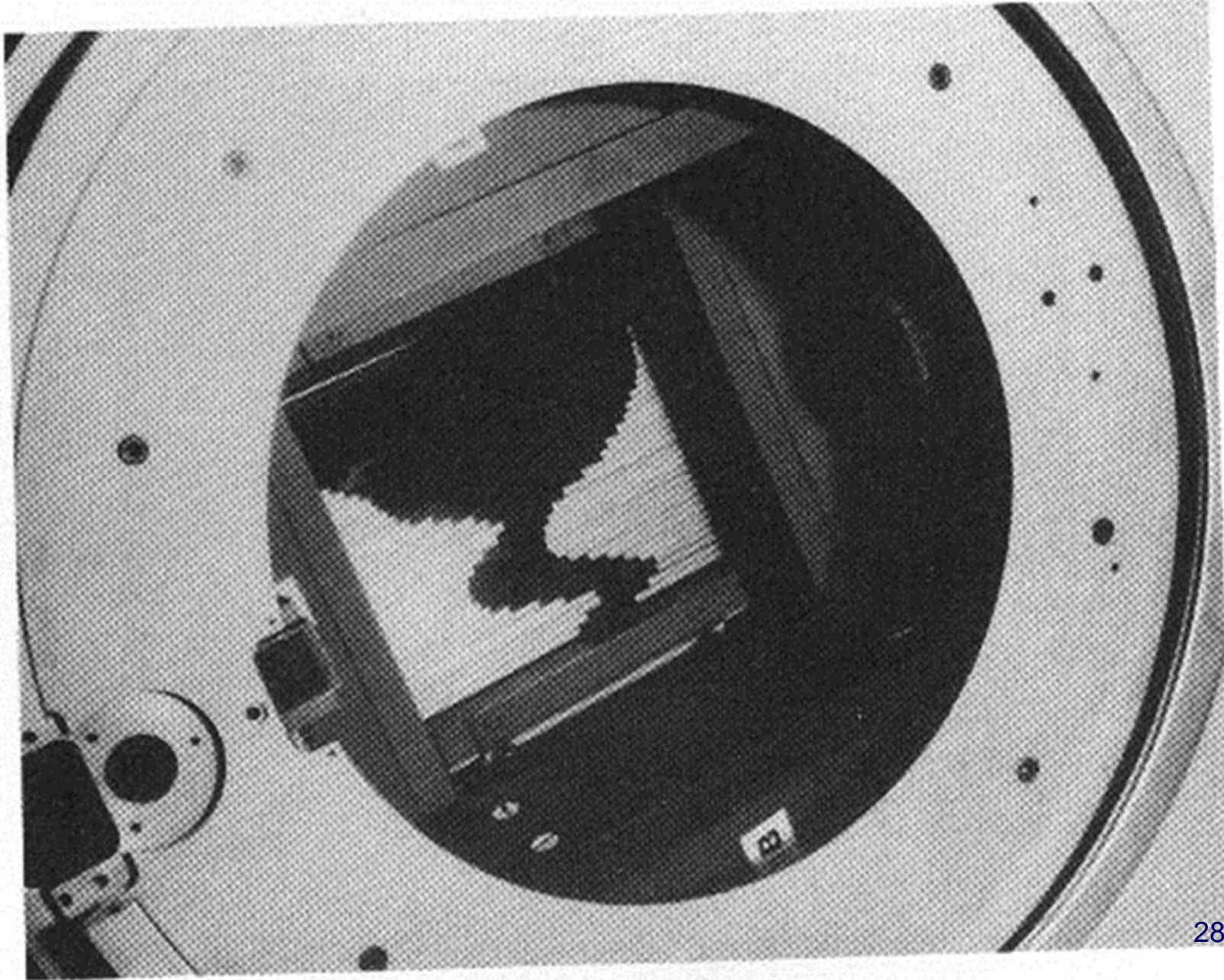
MLC: Tongue and Groove



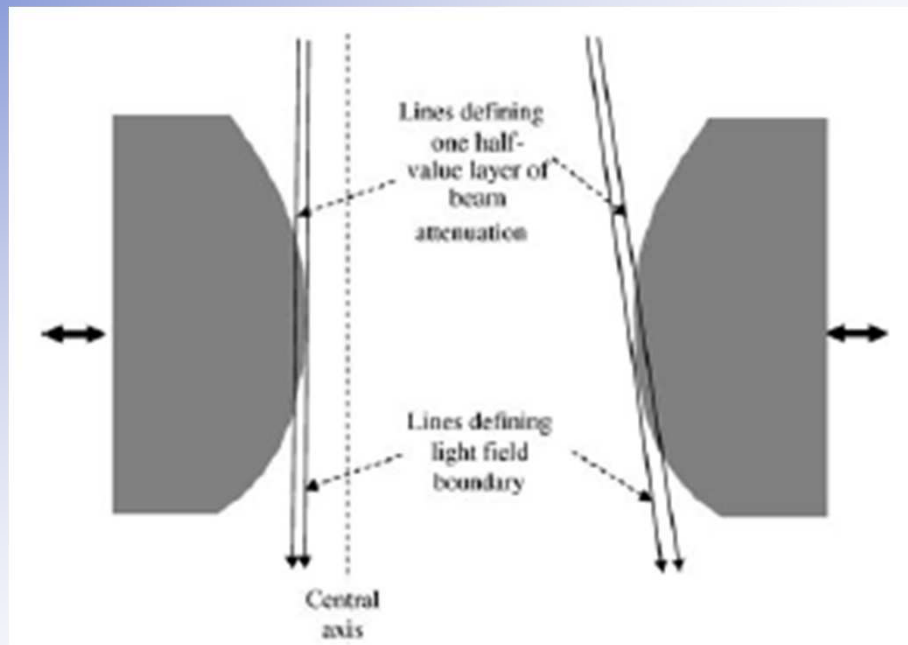
(a)



(b)



Curved leaf ends



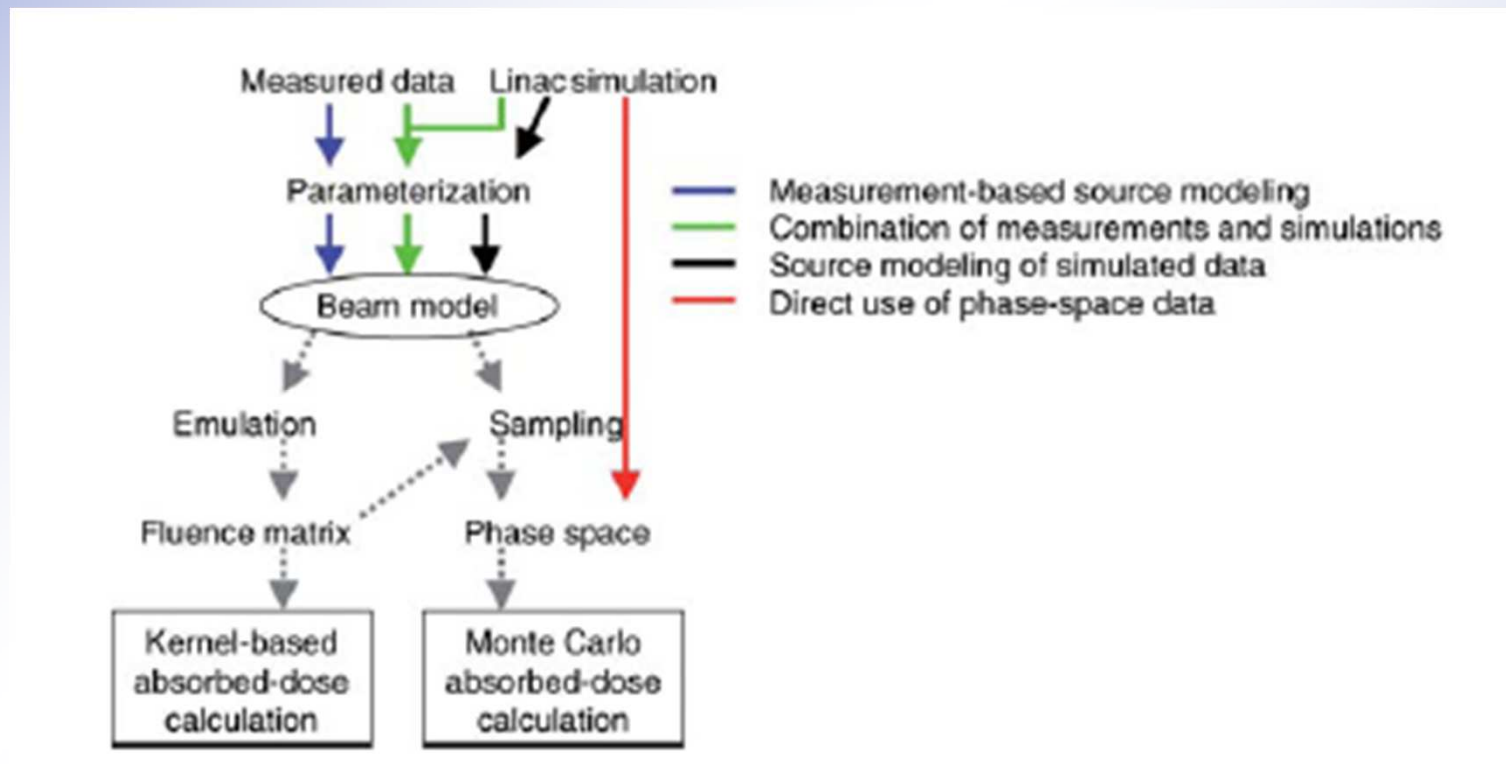
The effect of curved leaf ends

For reasons of mechanical simplicity, most conventional MLCs use simple linear motion (as indicated by the bold double arrows). Here, one leaf is shown close to the central axis and the other farther from the central axis. If the leaves were not curved, there would be a sharp transition in crossing the central axis where the light field would be defined first at the top and then at the bottom of the collimator. The use of curved leaf ends causes the edge of the light field to differ from to the edge of the radiation field, which is typically defined by one half-value layer of attenuation. The discrepancy between the boundary defined by the light field and the radiation field is not constant with leaf position, but varies with position across the field. There is also significant leakage through the leaves when the leaves are in the “closed” position. In the “closed” position, opposed leaves might not touch because there is usually a small gap between the leaves. Curved leaf ends also degrade the penumbra of the field and make beam modeling in this region more difficult.

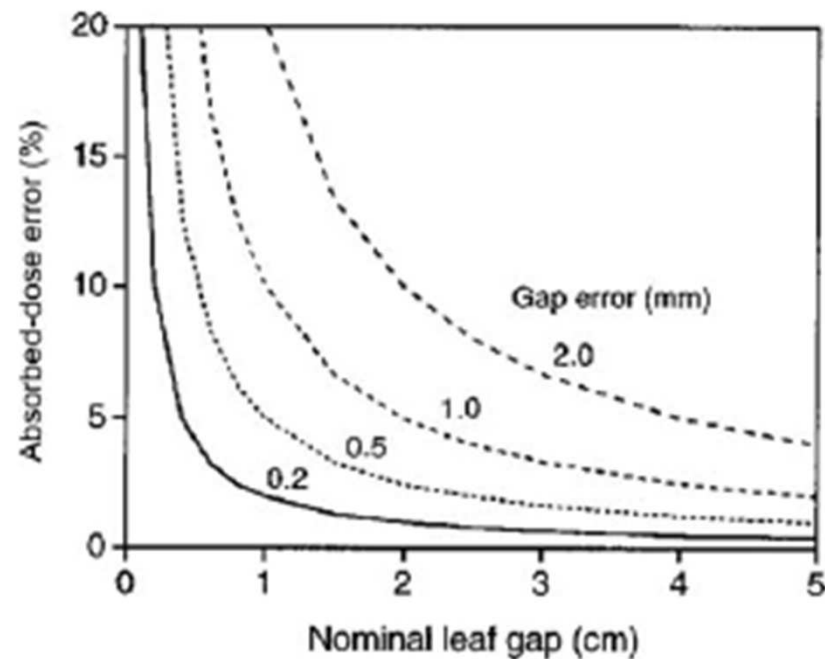
Video.mp4

Beam data

- Different beam data characterisation routes for absorbed dose calculations



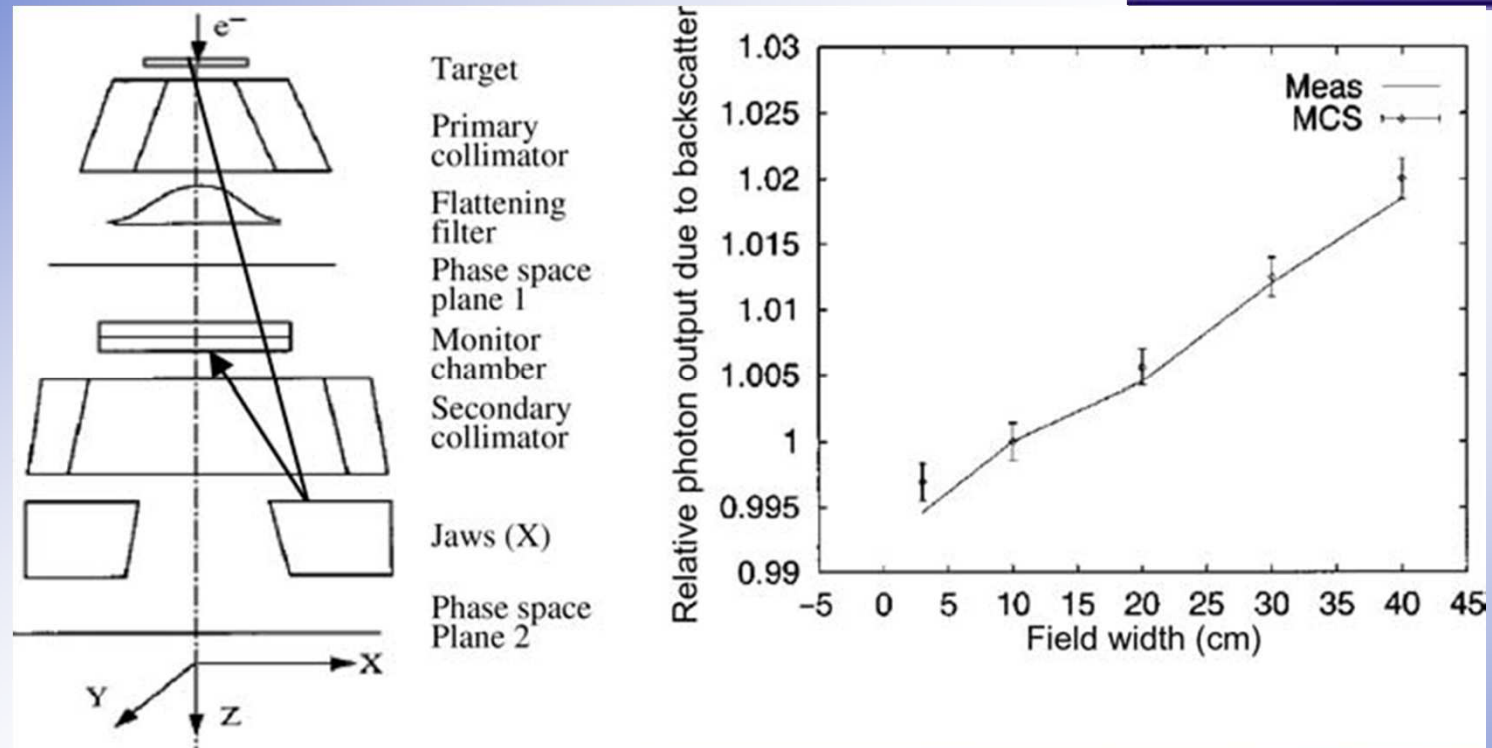
Leaf Gap and IMRT



Curves showing the increasing absorbed-dose error with decreasing nominal leaf gap (leaf-gap setting). The nominal leaf gap is the spacing between pairs of leaves that form the moving aperture of a dynamic MLC delivery.

LoSasso, T., Chui, C. S., and Ling, C. C. (1998). "Physical and dosimetric aspects of a multileaf collimation system used in the dynamic mode for implementing intensity modulated radiotherapy," Med. Phys. 25, 1919-1927.

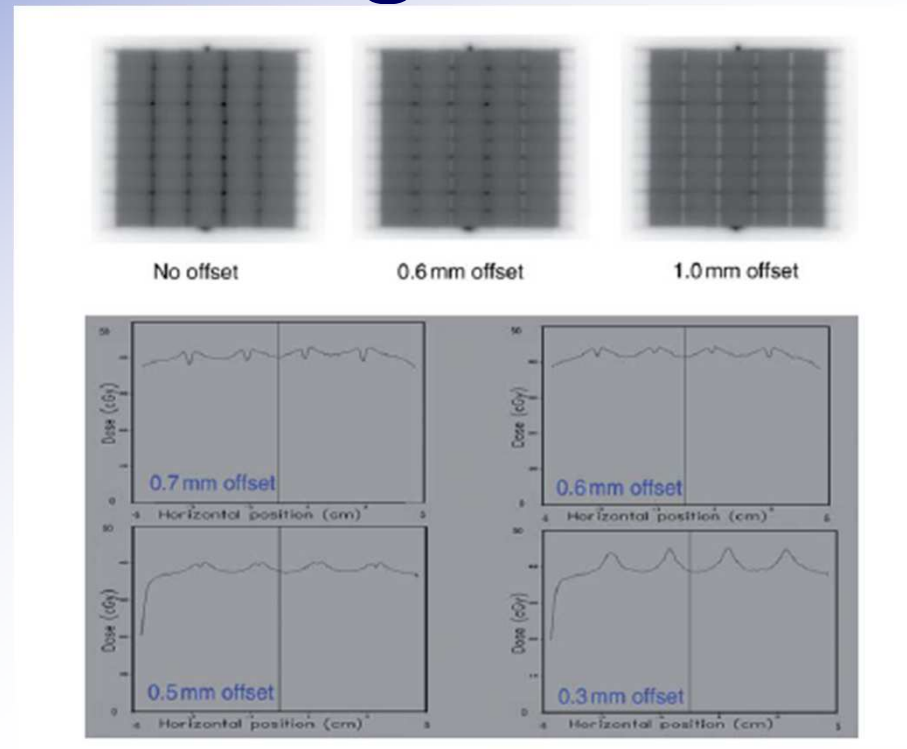
Back scatter and feedback



The effect of photon backscatter into the monitor chamber for a 10 MV photon beam. Monitor chambers can provide feedback to stabilize the output of a linear accelerator. When the field size is changed by moving the collimators defining the field (jaws), the backscatter into the monitor chamber changes (see left panel). Increasing backscatter lowers the output per unit monitor unit of the linac correspondingly. The amount of backscatter as a function of square-field size is a few percent (see right panel). This effect should be included in the monitor-unit calculations.

Liu, H. H., Mackie, T. R., and McCullough, E. C. (2000). "Modeling photon output caused by backscattered radiation in the monitor chamber from collimator jaws using a Monte Carlo technique," Med. Phys. 27, 737-744.

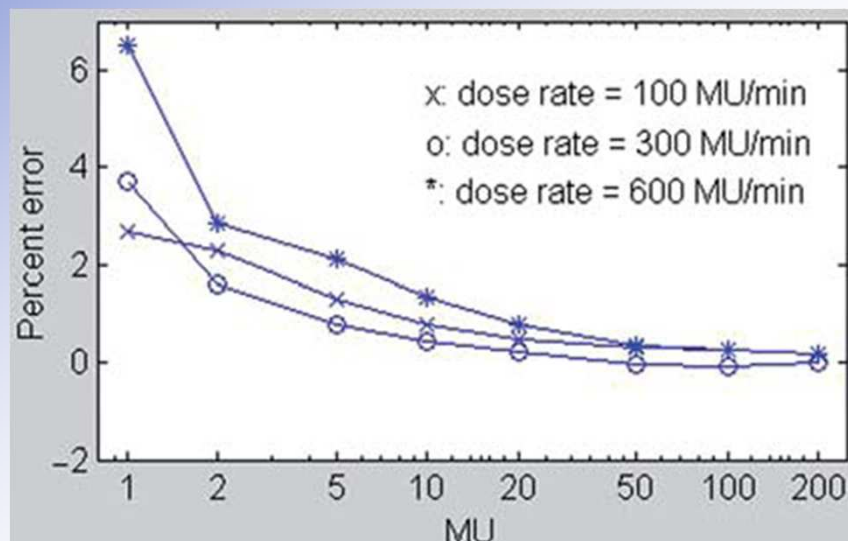
Leaf gap offset test – IMRT Comissioning



Test to determine the optimal leaf-gap offset due to the curved leaf ends on a conventional MLC. A 10 cm 10 cm field is formed by five successive irradiations of 2 cm 10 cm field strips as shown in the upper panel, where the thin horizontal stripes are due to inter-leaf leakage. With zero offset between the strips, there is a hot junction (due to leaf leakage through the curved leaf ends) between the strips as indicated by the vertical black stripes between the strips. With a 1.0 mm offset, there is a cold junction between the strips as indicated by the vertical white stripes. In the lower panel, the offset is varied between strips to minimize both the hot and cold spots. The ideal offset is between 0.5 mm and 0.7 mm, which implies that the accuracy of the test is about +0.1 mm.

IMRT Commissioning

- MU linearity



Measurement of the error that can result when a small number of monitor units (MUs) are delivered multiple times. The abscissa represents MU per delivery. After each delivery, the beam is turned off. In all tests, a total of 1000 MU was delivered. Unlike conventional radiotherapy, small numbers of MUs are often delivered for different segments in IMRT. The error is generally larger for small numbers of MUs delivered at high absorbed-dose rates.

Palta, J. R., Kin, S., Li, L. G., and Liu, C. (2003). "Tolerance limits and action levels for planning and delivery of IMRT," pp. 593–612 in Intensity-Modulated Radiation Therapy: The State of the Art, Palta, J., and Mackie, T. R., Eds. (American Association of Physicists in Medicine, College Park, MD).

MLC leaf calibration

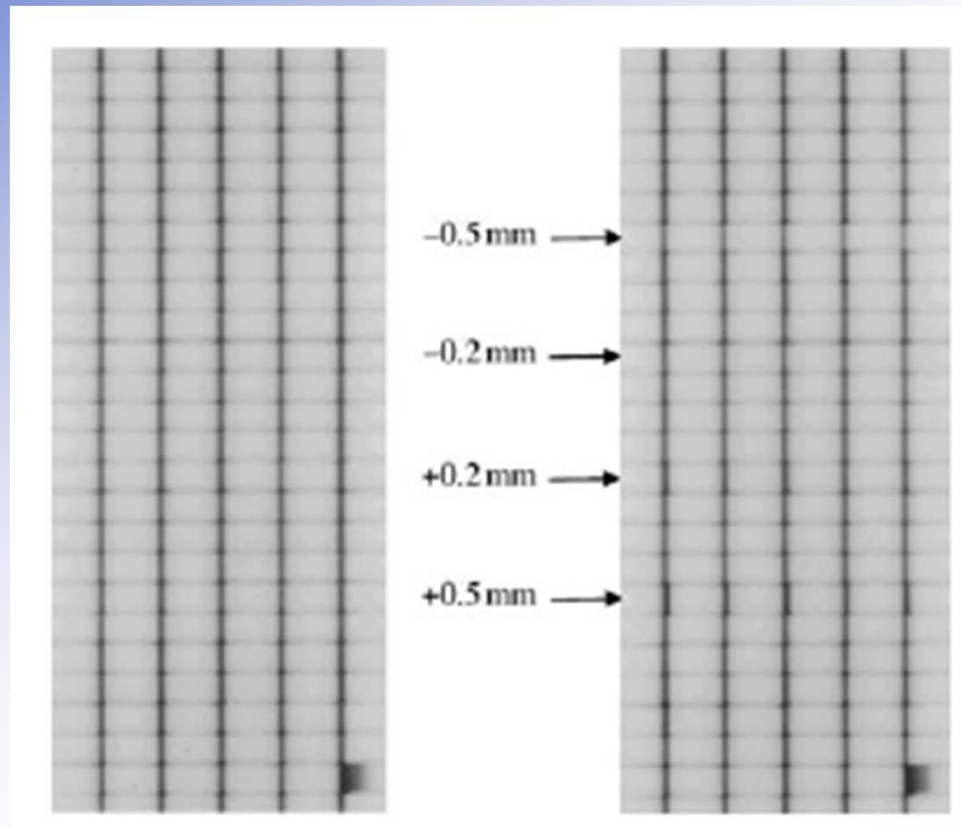


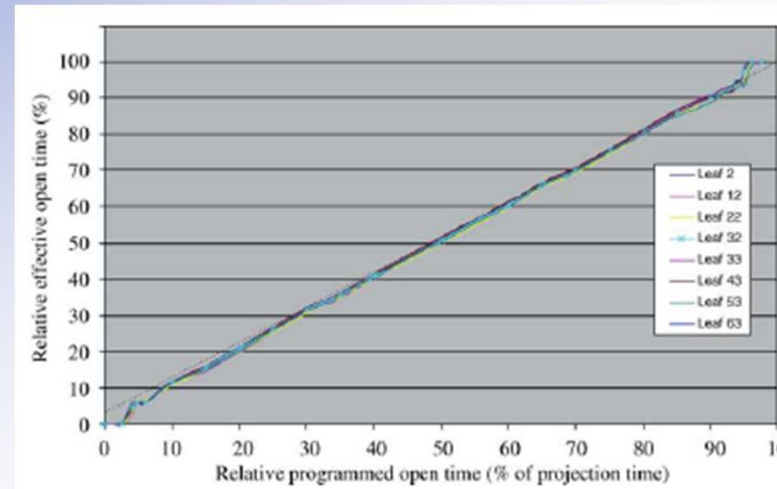
Illustration of a test to determine correct leaf calibration. A series of 1 mm wide leaf irradiations are delivered to radiographic film at multiple positions across a field. On the left is an illustration of correct leaf-position calibration. On the right is an illustration of purposely set leaf errors to illustrate the sensitivity of the test. Leaves that are offset by 0.5 mm can be detected, but offsets of 0.2 mm cannot be detected with this test. The leaf on the right, second from bottom, has been purposefully offset halfway across the gap to mark the film with respect to orientation, and it is possible to see the differential transmission through the curved leaf end with more leakage through the left part of the gap and less transmission through the right part.

Tomotherapy commissioning



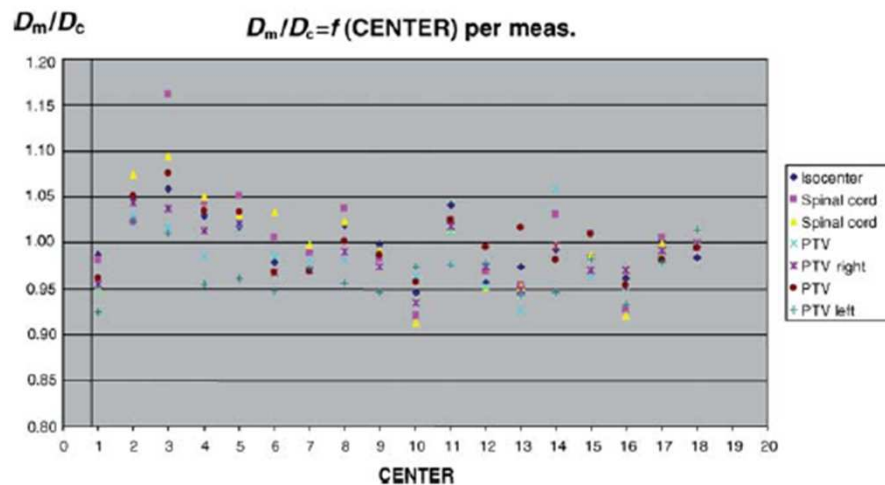
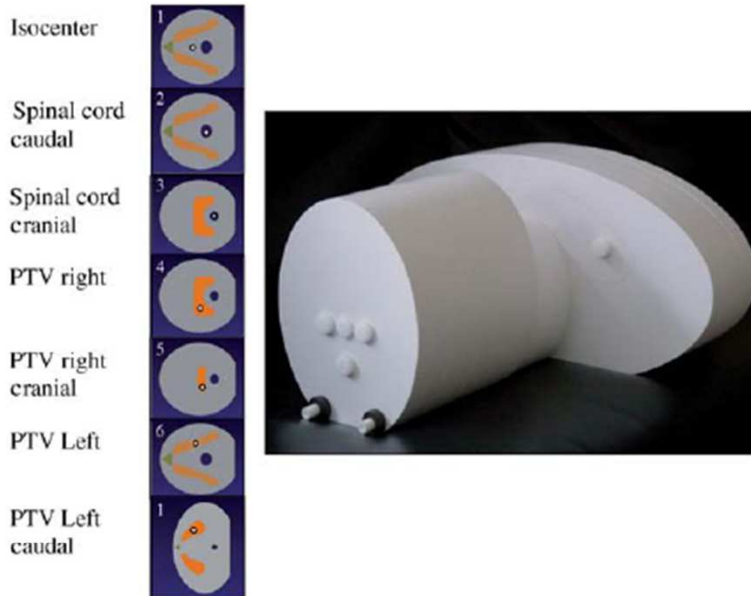
The fluence-output factor (FOF) as a function of leaf number for the TomoTherapy Hi-Art™ system. The measured increase in energy fluence when both neighboring leaves are open is called the FOF. The figure shows the variation in FOF as a function of leaf number. Two runs of the test, listed as FOF1 and FOF2, are shown together with the average results. If only one neighboring leaf is open, the increase in energy fluence is half of the increase shown. The variation from leaf to leaf is due to small (of the order of 25 mm) variations in mechanical precision of the fixture holding the leaves. The asymmetry is due to a lateral offset in the MLC. Calibration of the FOF enables the MLC to operate with wider mechanical tolerances. (Figure courtesy Tomo Therapy Inc., Madison, WI, USA)

Tomotherapy commissioning



Binary collimator leaf-performance information used for monitor-unit calculations on the Hi-Art™ helical tomotherapy unit. This figure shows the effective open time as a percentage of the time for one projection, here 500 ms long, for binary leaves when compared with their programmed open-time request. In helical tomotherapy, a single rotation is divided into 51 arc segments called projections; a projection lasts a time equal to the time for one complete rotation divided by 51. The programmed relative open time (%) is varied from very small values to the full projection time of 500 ms, and the time that the leaf is actually open is determined by processing of the megavoltage x-ray detector signal. The x-ray detector acquires a reading for every channel for every linac pulse, allowing a temporal resolution of about 3 ms or about 0.6 % of the projection time to determine when the leaves are opened or closed. The control of the leaves is such that all of the leaves at the beginning of a projection are closed. The finite leaf opening and closing time prevents a leaf from achieving a relative opening time greater than about 95 %. To deliver a very small opening time, a leaf has to begin to open and, then before it is fully open, it must start to close. It can be seen that relative opening times less than about 5 % are not possible. The dynamic range of modulation for a binary collimator controlled in this manner is continuous but with a range smaller than the projection time. The curves, one for each leaf listed, are nearly superimposed indicating similar opening and closing times. A dashed line indicates a line defining equal requested and effective open times. This measured performance of individual leaves is used in the monitor-unit calculation to determine what the leaf opening times should be. (Figure courtesy of TomoTherapy Inc., Madison, WI, USA)

Phantom Measurements for IMRT



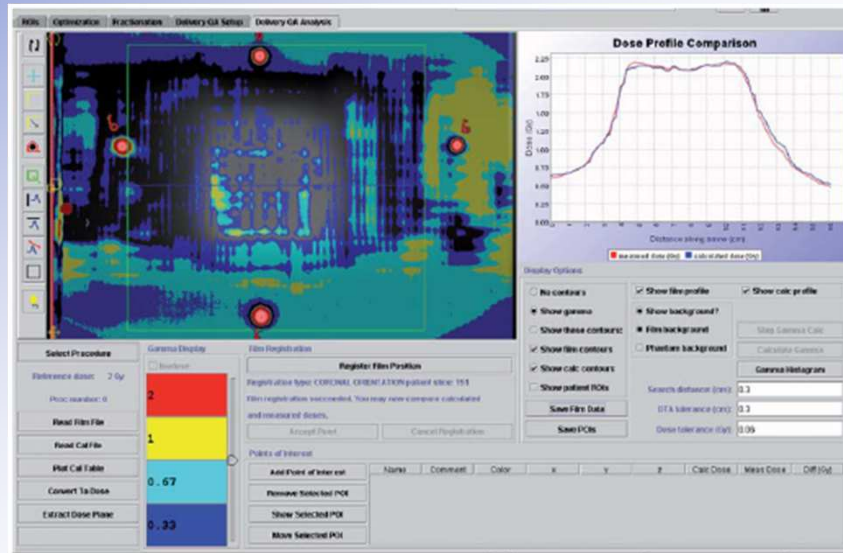
Upper panel is the phantom developed by the GORTEC to compare the ratio of the measured absorbed dose to the computed absorbed dose at several positions for head-and-neck radiotherapy. The orange regions of interest indicate the target volume on each of the slices. About 20 % of the 126 TLD measurements from 18 centers did not agree within 5 % of the treatment-planning calculations. The spread of measurements within a center was much less than the spread of measurements between centers. (Figure courtesy of Milan Tomsej, St. Luc University hospital, Brussels, Belgium.)

IMRT Methods



Type of method	Intensity modulation method	Preferred optimization approach
Compensators	A beam filter designed to provide a patient-specific intensity pattern designed by an optimization procedure	Optimized beamlets
Segmental MLC (step and shoot)	Multiple MLC segments delivered from each treatment direction	Direct-aperture optimization
Dynamic MLC (sliding window)	Leaves slide across the field at different rates	Optimized beamlets
Intensity-modulated arc therapy (IMAT)	Leaves move while the gantry is rotating. Can require multiple rotation arcs	Direct-aperture optimization
Serial tomotherapy	Gantry rotates around the patient with the couch fixed. Binary leaves modulate a fan beam. Upon completion of each rotation, the couch is moved in a step-wise fashion	Optimized beamlets
Helical tomotherapy	Gantry and couch move synchronously. Binary leaves modulate a fan beam	Optimized beamlets
Robotic radiotherapy	Multiple non-coplanar pencil beams delivered by a robot	Optimized beamlets

Gamma Map



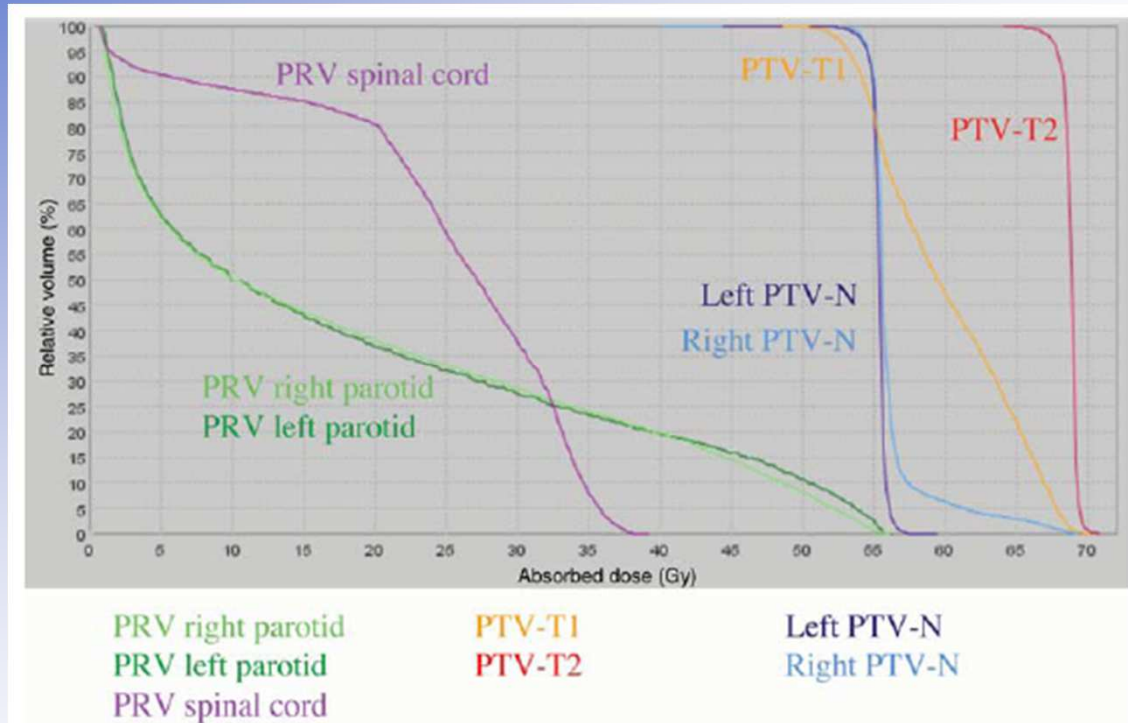
A gamma map of a comparison between a computed absorbed-dose distribution and film measurements for a helical tomotherapy absorbed-dose distribution in a cylindrical phantom. The criteria selected were $DdM \frac{1}{4} 3$ mm (DTA) and $DDM \frac{1}{4} 3$ % (absorbed-dose difference), which corresponded to a 0.0006 Gy absorbed-dose difference. The color scale indicates the relative gamma values. Black corresponds to a gamma value below 0.33; dark blue corresponds to a gamma value above 0.33 but less than 0.67; light blue corresponds to a gamma value above 0.67 and below or equal to 1; yellow corresponds to gamma values above 1 but below or equal to 2; red corresponds to gamma values greater than 2. An absorbed-dose profile comparing the calculated and measured values is also shown. The profile indicates that the calculated and measured values agree well inside the field except near the left boundary, which has a gamma value above 1. The four circular regions are due to pin marks placed on the film for purposes of alignment.

ICRU 83 (2010)

As introduced in ICRU Reports 50, 62, 71, and 78 (ICRU, 1993; 1999; 2004; 2007)

- Gross tumor volume or GTV
- Clinical target volume or CTV
- Planning target volume or PTV
- Organ at risk or OAR
- Planning organ-at-risk volume or PRV
- Internal target volume or ITV
- Treated volume or TV
- Remaining volume at risk or RVR

Dose Volume Histogram (DVH)

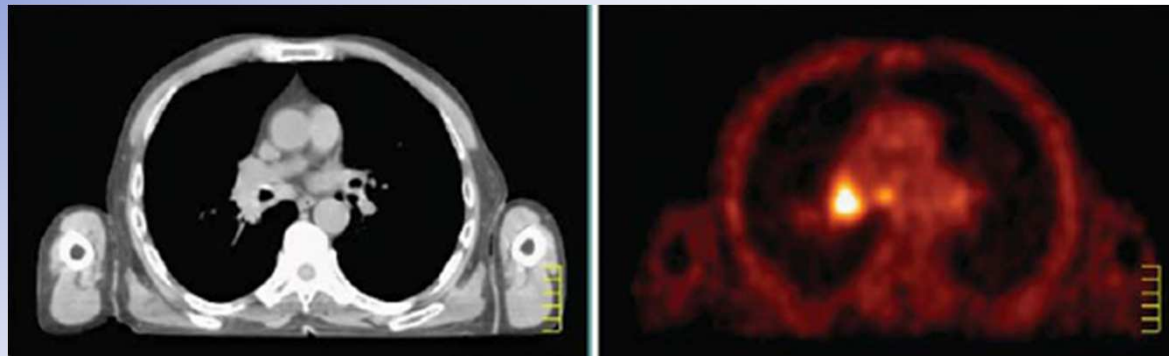


ICRU 83
(2010)

Comparison of dose–volume histograms (DVHs) for the various PTVs and PRVs for Case B1. The relative volumes are normalized to the total volumes of the region of interests and expressed as percent. The various absorbed-dose metrics derived from these DVHs are reported in Table B.1.2. The large difference between the DVH for PTV-T2 and PTV-T1 is not so apparent in the section presented in Figure B.1.4. The section refers to an absorbed-dose distribution in a plane and does not necessarily reflect the absorbed-dose distribution in a volume. Appendix B: Clinical Examples 85

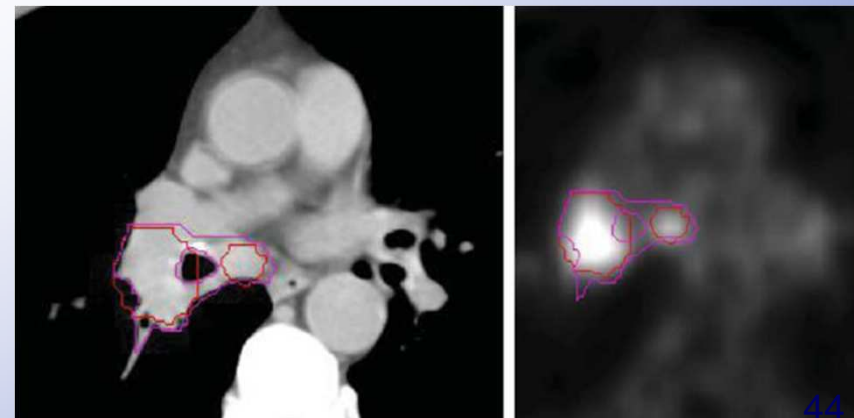
Target delineation

Transverse CT (left) and FDG-PET (right) slices showing tumor in the left hilus with a lymph node in region VII

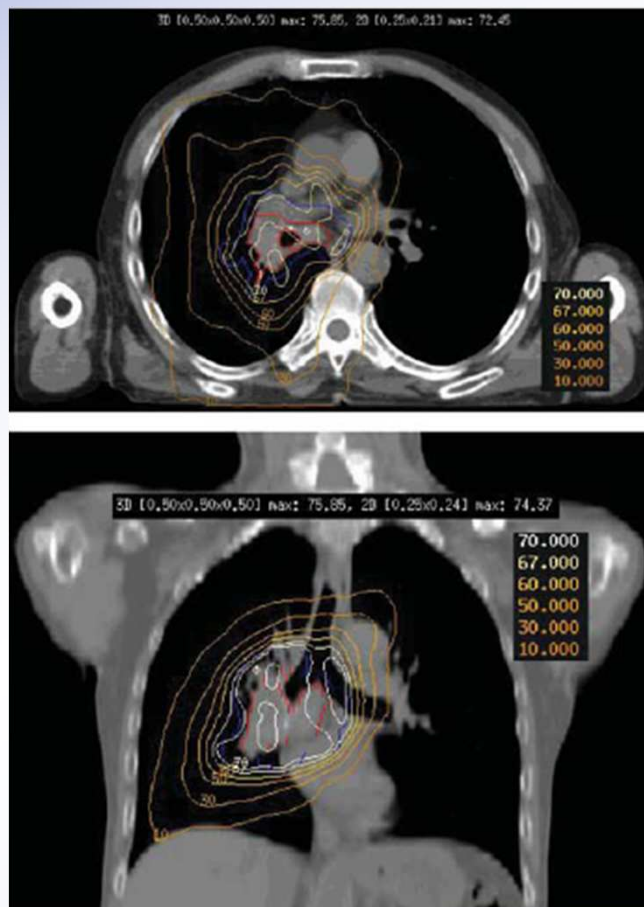


Gross tumor volume delineated on CT (left panel) using an automatic gradient-based delineation of the FDG-PET images (right panel). The GTV-T (FDG-PET, 0 Gy) and GTV-N (FDG-PET, 0 Gy) are displayed in red; the GTV T p N (FDG-PET p CT, 0 Gy) is displayed in pink in both panels.

25 September 2010



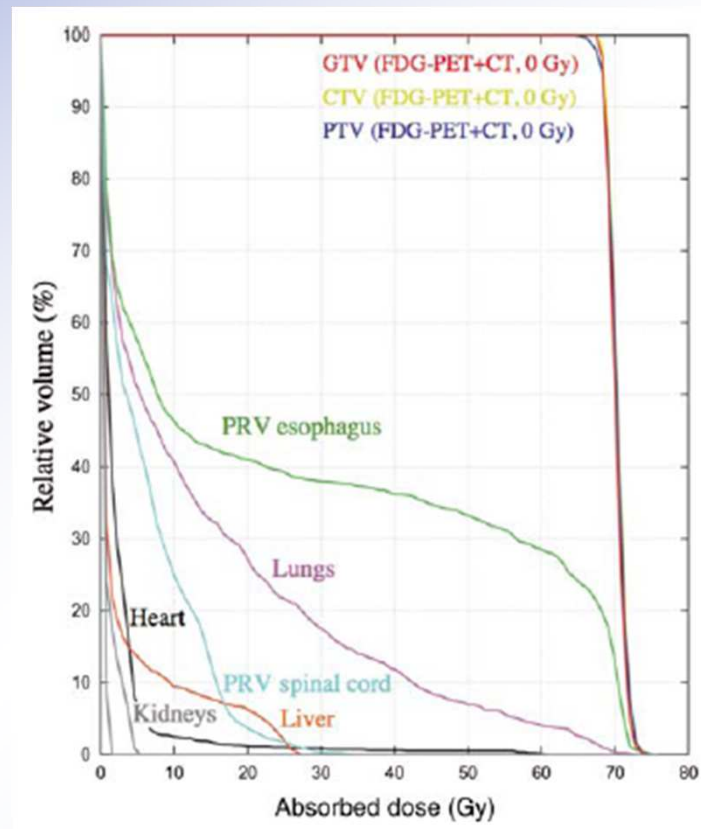
Dose distribution



**ICRU 83
(2010)**

Figure B.2.3. Isodose distribution on transverse (top panel) and coronal (bottom panel) sections. The GTV-T + N (FDG-PET + CT, 0 Gy) is delineated in red; the PTV-T + N (FDG-PET + CT, 0 Gy) is delineated in blue.

Cumulative DVHs



**ICRU 83
(2010)**

Figure B.2.4. Cumulative DVHs for the PTV, CTV, GTV, OARs, and PRVs for Case B2. The various absorbed-dose metrics derived from these DVHs are reported in Table B.2.3.

B.3 Case Number B3. Adenocarcinoma of the Prostate

Figure B.3.2. Axial image at the center of the PTV, with isodose distributions (in Gy).

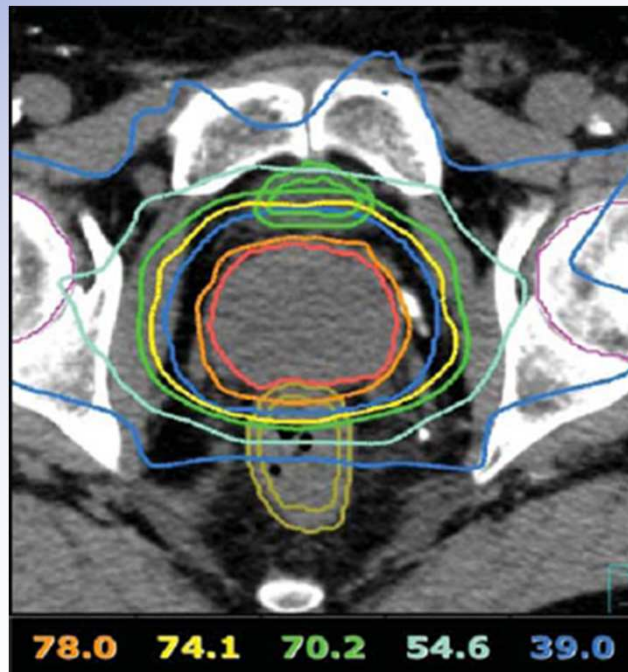
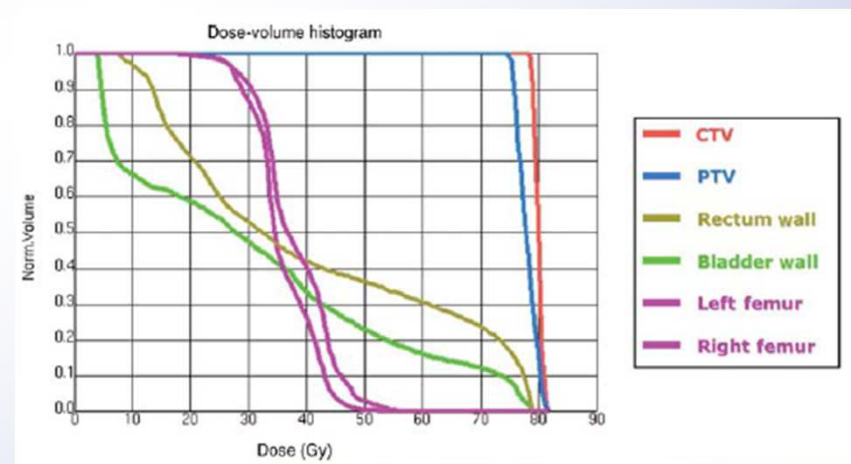


Figure B.3.3. Comparison of DVHs for the PTV and OARs for Case B3. The various absorbed-dose metrics derived from these DVHs are reported in Table B.3.2.



ICRU 83
(2010)

B.3 Case Number B3. Adenocarcinoma of the Prostate



Planned and reported absorbed-dose metrics for CTVs, PTVs, OARs, and PRVs for Case B3.

Volume	$D_{\text{near-min}}$ or $D_{98\%}$ (Gy)	$D_{50\%}$ (Gy)	$D_{30\%}$ (Gy)	$D_{\text{near-max}}$ or $D_2\%$ (Gy)
PTV	74.1 (≥ 74.1) ^a	78.0	—	81.5 (<81.9)
CTV	78.6	—	—	81.5
PRV rectal wall	—	32.2 (55.0)	60.5 (70.0)	78.7 (79.0)
PRV bladder wall	—	27.6 (55.0)	42.5 (70.0)	78.1 (79.0)
PRV left femur	—	—	—	46.5 (53.0)
PRV right femur	—	—	—	51.3 (53.0)

^aThe planning-aim absorbed doses are given in parenthesis.

TABLE 1. CLASSIFICATION OF CONFORMAL THERAPY ACCORDING TO THE METHODOLOGY AND TOOLS ASSOCIATED WITH EACH STEP OF THE PROCEDURE

	Level 1 Basic CRT	Level 2 3-D CRT	Level 3 Advanced 3-D CRT
1. Patient data acquisition			
Immobilization	Desirable	Customized to the patient	Customized to the patient
Imaging system	Localization films, few CT slices optional	Thin adjacent CT slices, MR optional	Co-registered CT with MR or PET
Anatomical data			
Reference marks for setup	Height above table and skin marks	External markers or frame	Implanted markers or frame
Critical organs	Contour individual slices	3-D segmentation	3-D segmentation
Inhomogeneities	Optional	Contouring every slice or voxel based correction	Voxel based correction
Gross tumour volume (GTV)	May not be formally defined	Contouring every slice	3-D segmentation
Clinical target volume (CTV)	May not be formally defined	Grown from GTV using auto-margin growing	Margin growing from GTV + functional imaging
Internal target volume (ITV)	May not be formally defined	Based on standard decision rules	4-D CT data to define ITV customized to patient
2. Beam definition			
Accounting for beam setting uncertainty	Margins are not customized	3-D margins based on audit of setup errors	Image guidance
Type of radiation and beam modifiers	Photons or electrons \pm wedge filters	Photons, wedges, field in field, compensators	Photons + IMRT
Beam incidence	Coplanar beams	Several (including non-coplanar) beams	Multiple non-coplanar beams or arcs
Isocentre	SSD or SAD technique	SAD technique (auto centred on target)	SAD technique (auto centred on target)
Beam limiting device	Non-customized shielding blocks	Customized blocks or MLC	MLC or mini MLC
PTV – CTV margin	Shape drawn on simulation films	Protocol margins based on audit	Individual margin based on e.g. 4-D CT
3. Dose calculation and optimization			
Calculation model	1-D or 2-D (slice) \pm inhomogeneity	2-D or 3-D with inhomogeneity	3-D or 4-D with inhomogeneity
Evaluation of treatment plans	Isodoses on central slice or several slices	Isodoses viewed in 3-D on computer + DVH	3-D isodose surface + DVH, TCP, NTCP
Treatment plan optimization	Successive trials + visual appreciation	Successive trials + simple optimisation	Inverse planning
4. Treatment verification and execution			
Verification simulation	Normal practice	Useful	Replaced by IGRT on treatment machine
Immobilization (see above)	Desirable	Customized to the patient	Individual cast or stereotactic frame
Aids for positioning	Lasers + light field	Isocentre lasers	Lasers or frameless stereotaxy
Patient positioning	Height above couch + skin marks	Move from anatomical reference or stereotaxy	Daily image guidance
Verification reference image	Simulation film	DRR	CT data compared to cone beam CT
Record and verify system	Desirable	Essential but network is optional	Essential including network transfer
In vivo measurements	Desirable	TLD or diodes recommended	TLD or diodes or EPID transit dosimetry



HEMALATA
HOSPITALS AND
RESEARCH CENTRE

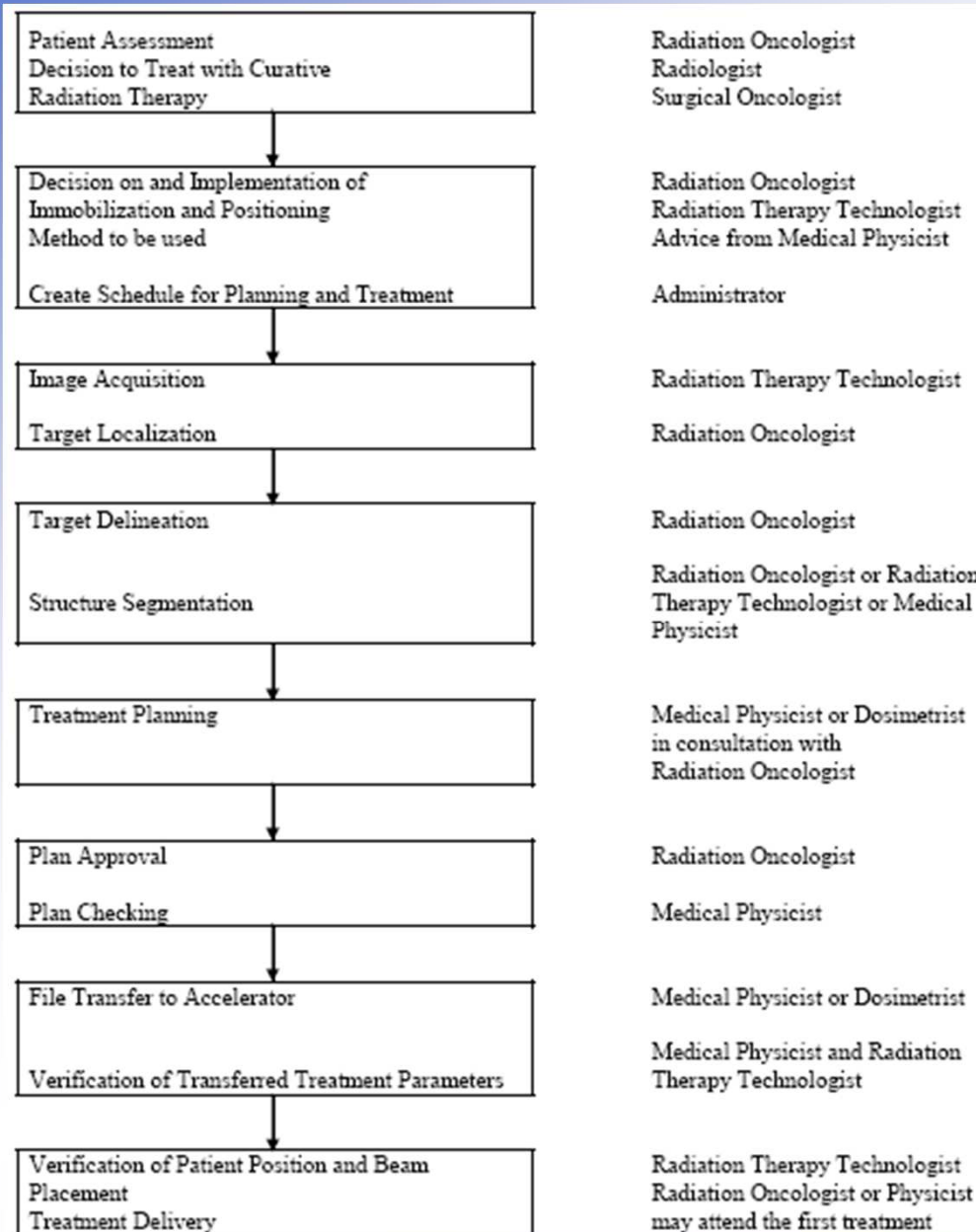
IAEA-TECDOC-1588

*Transition from 2-D Radiotherapy to
3-D Conformal and Intensity
Modulated Radiotherapy*



May 2008

A typical 3-D CRT Process.



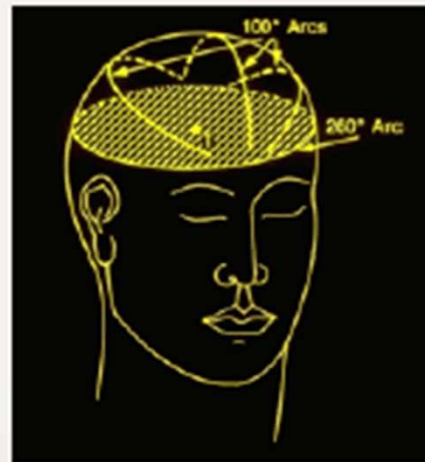
The right column shows the staff involved in each step.

STEREOTACTIC RADIOSURGERY

- Example of circular collimator attached to the linac head.



Multiple non-coplanar converging arcs technique:



STEREOTACTIC RADIOSURGERY



Comparison: Gamma Knife versus isocentric linac

	Gamma Knife	Isocentric linac
Radiation quality	201 cobalt sources	x rays (6-18 MV)
Radiation beam	Stationary	Stationary or moving
Dose rate	Up to 350 cGy/min	Up to 600 cGy/min
Fields	Circular	Circular or irregular
Field diameters	4, 8, 14, 18 mm	5 - 40 mm
Irregular fields	Not available	Produced with microMLC
Operation	Dedicated	Used for standard RT

The general consensus among radiation oncologists and medical physicists is that:

- Linac-based radiosurgery with regard to treatment outcome is equivalent to that provided by a Gamma Knife
- Linac-based radiosurgery, in comparison with Gamma Knife radiosurgery, is considerably more complicated but has a much greater potential for new and exciting developments.

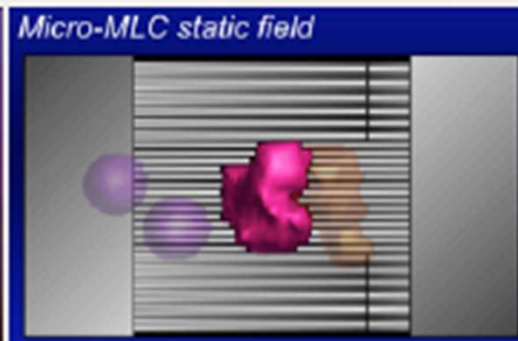
The general consensus among neurosurgeons is that Gamma Knife radiosurgery is superior to that practiced with isocentric linacs.

STEREOTACTIC RADIOSURGERY

The introduction of linac-based radiosurgery in radiation oncology departments during 1980s has rapidly transformed radiosurgery into a mainstream radiotherapy technique and has stimulated great advances in its technical and clinical utility.

- **Radiation oncologists** are quite comfortable with the clinical use of isocentric linacs but have reservations about the use of single high radiation doses in radiosurgery.
- **Neurosurgeons** had previous favourable experience with the Gamma Knife, but are concerned about the mechanical stability of linacs' isocentres.

Micro-MLC in linac-based radiosurgery

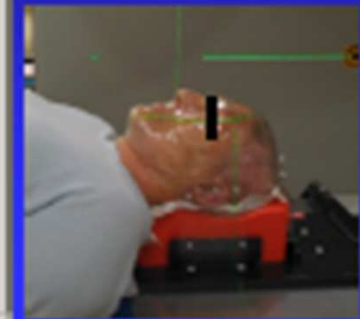
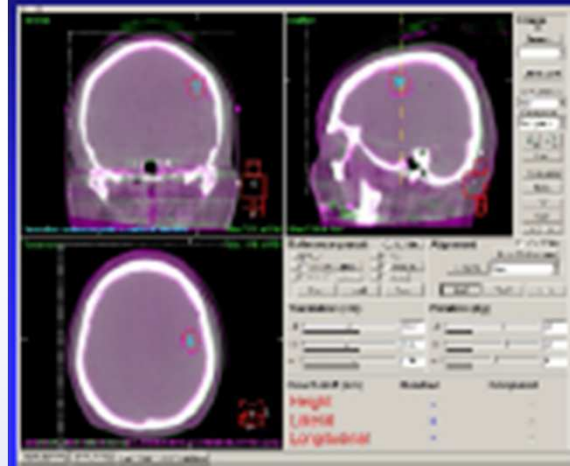


STEREOTACTIC RADIOSURGERY

With such a system, this is no longer needed to precisely irradiate a brain tumor



We can use this instead: focus on patient stability, but let computer position the patient with better than one mm precision



EVOLUTION OF RADIOTHERAPY



2D (pre 1990)

- Conventional Square/Rectangle
- Parallel Opposing
- Deep X-Ray / Cobalt-60

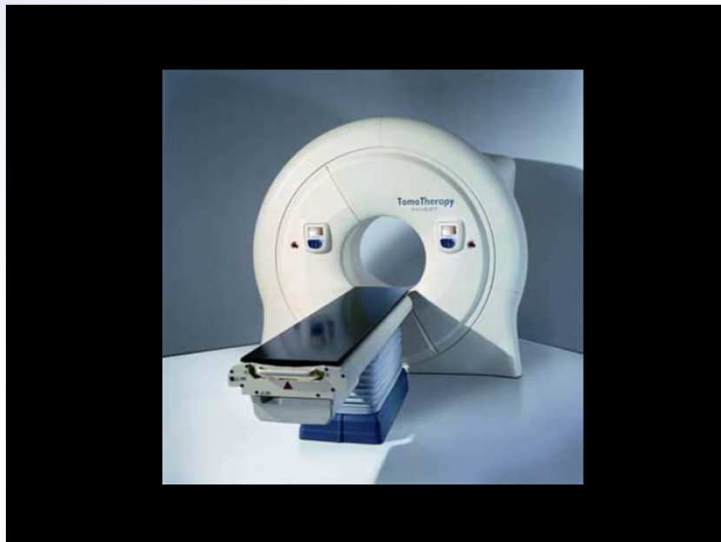
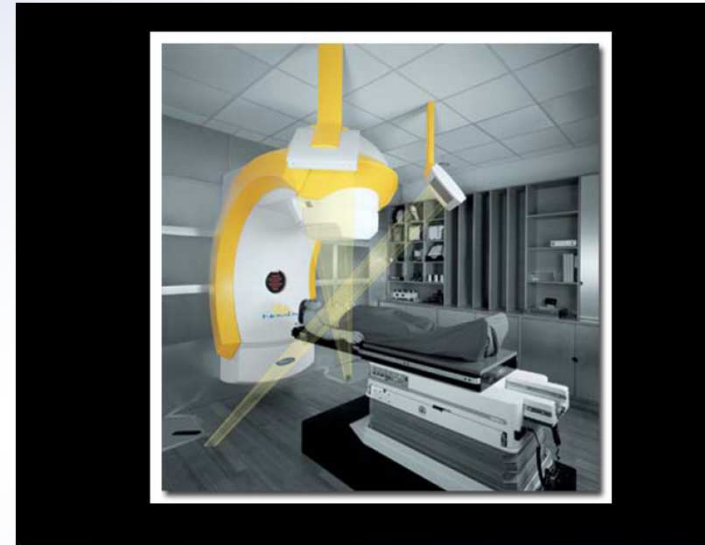
3D (post1990)

- Blocks, Multileaf Collimator
- Conformal RT,
- SRS/SRT, IMRT

4D(Today)

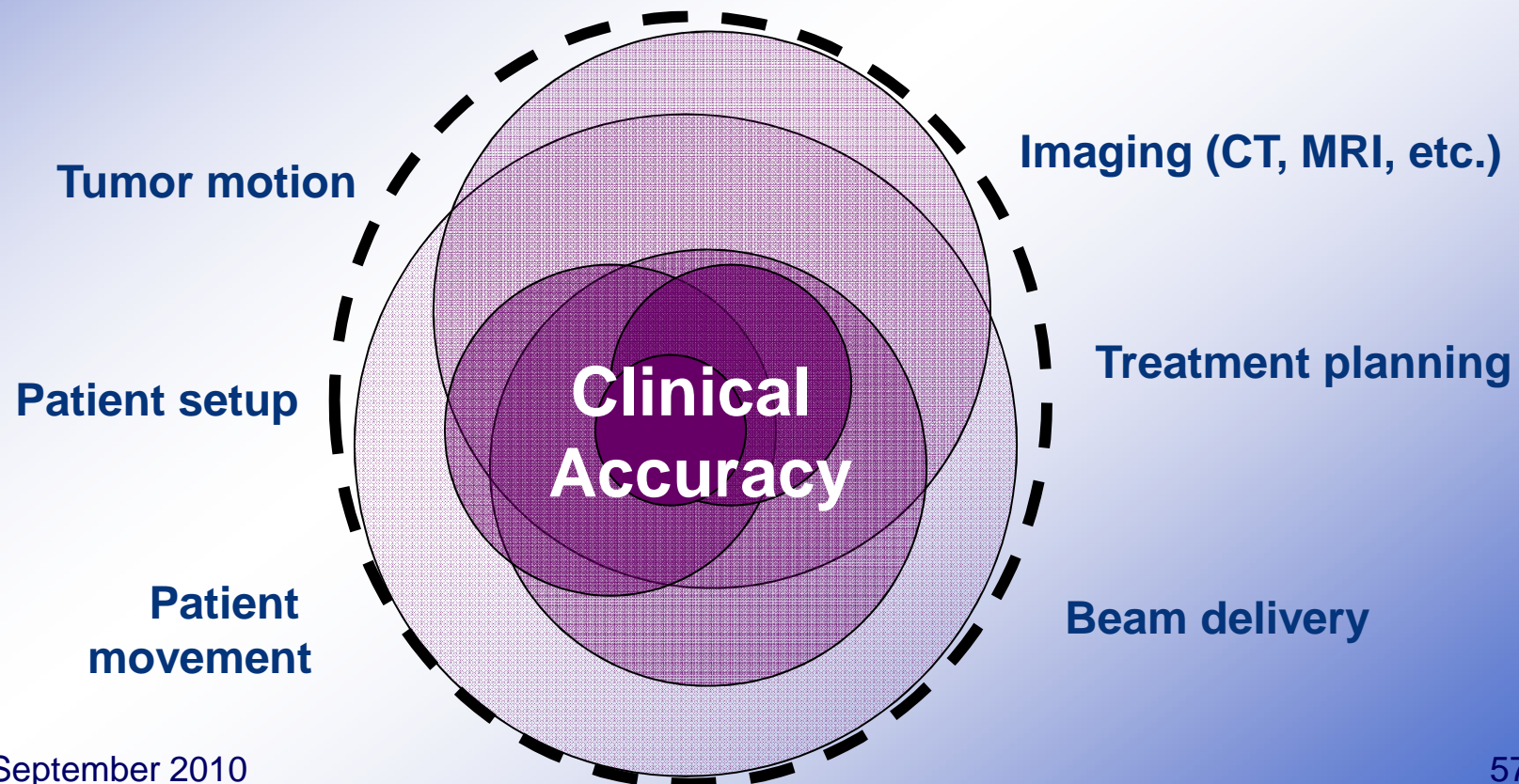
- Motion and Time Real Time with Feedback
- IGRT, Cyberknife Tomotherapy

Today's Radiotherapy

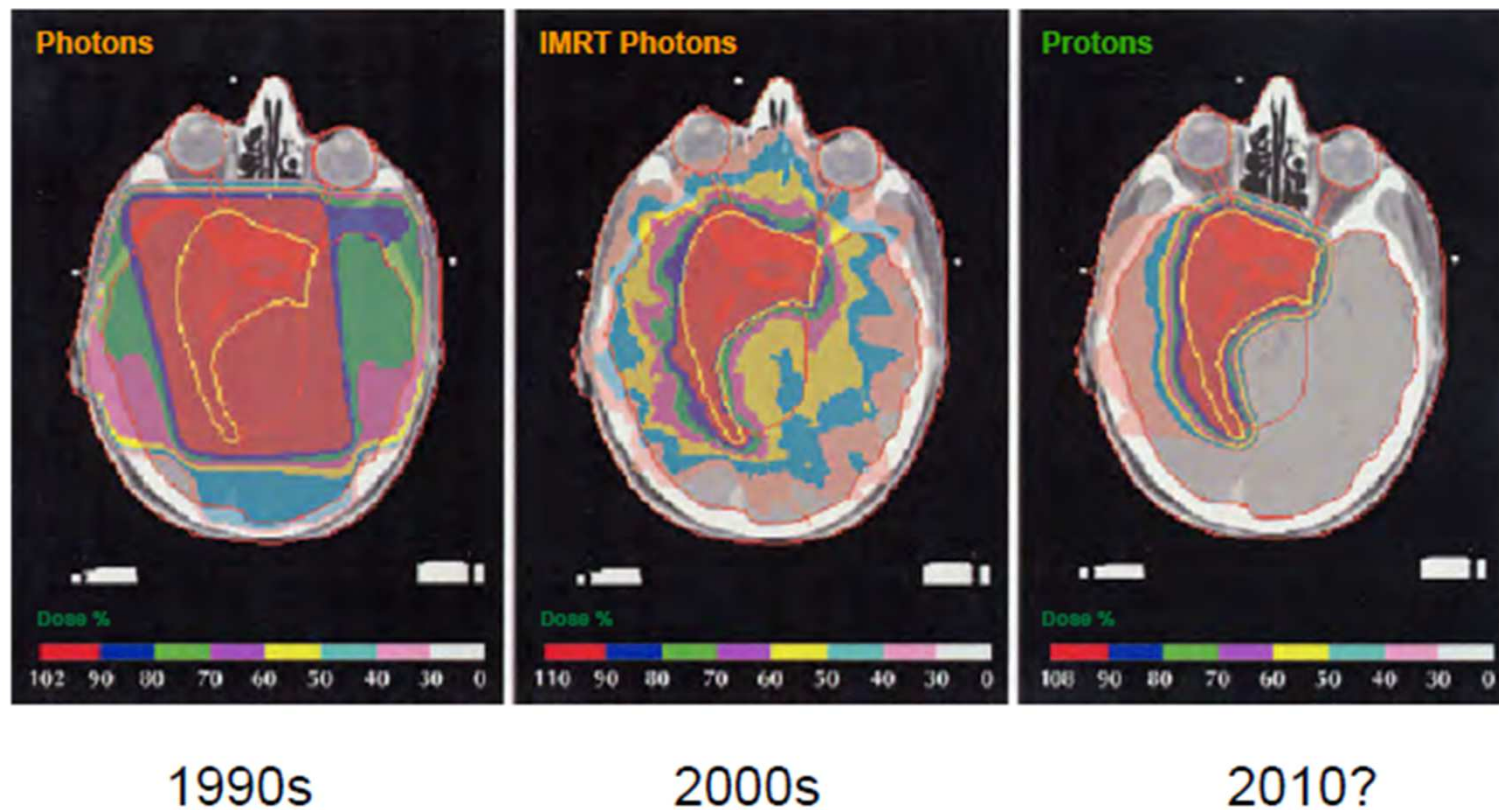


Precision in Radiotherapy

- Traditional Definition: Mechanical Accuracy
- New Definition: Clinical Accuracy

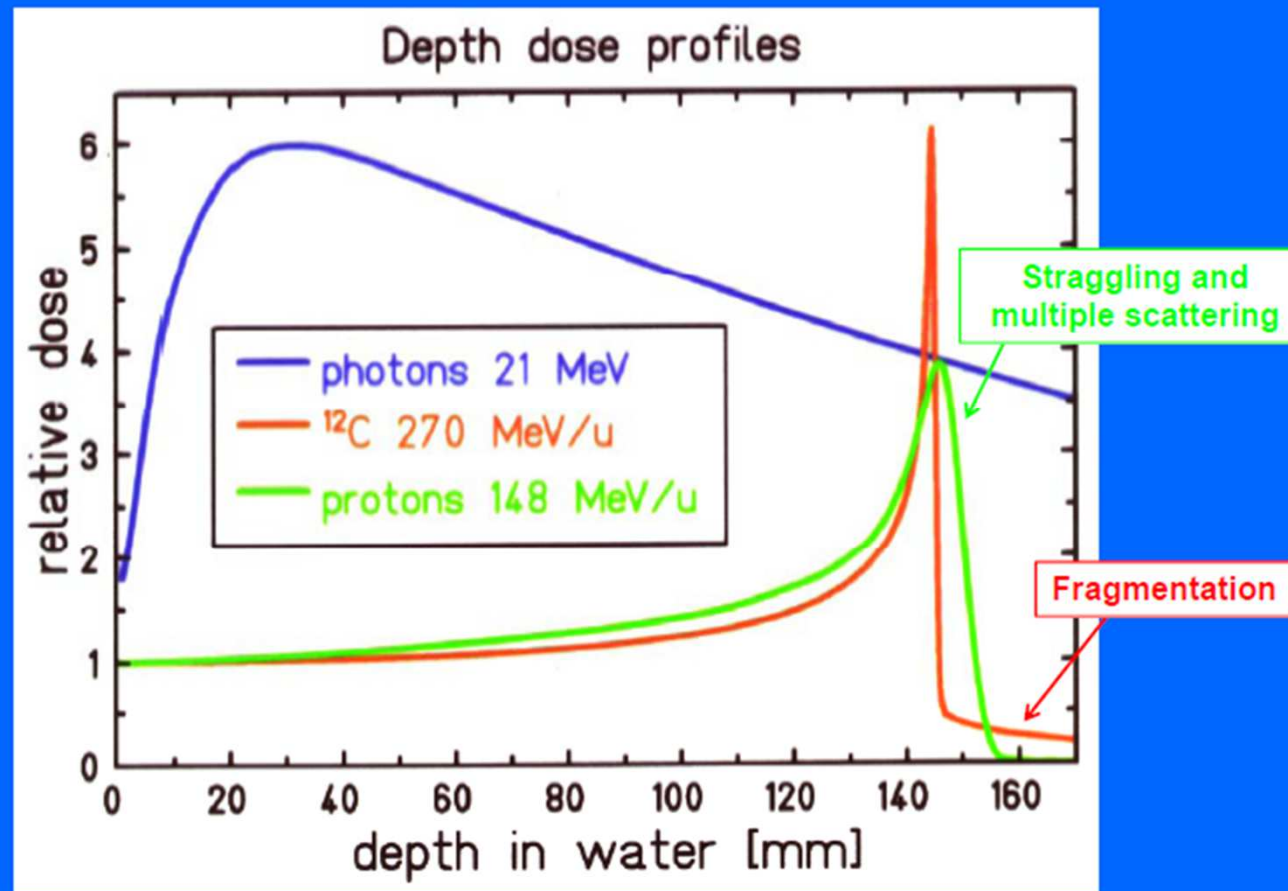


ADVANCES IN RADIOTHERAPY

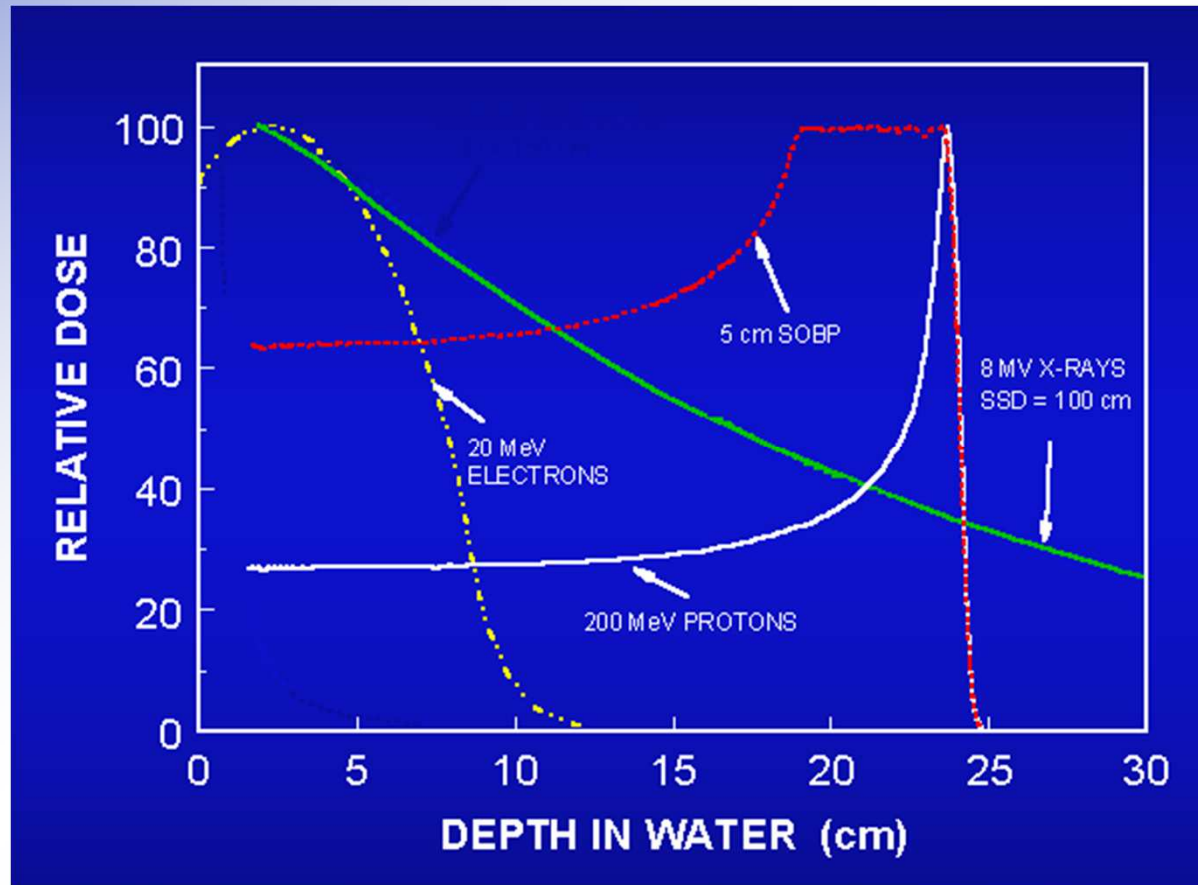


BEST FORM OF CONFORMAL RADIOTHERAPY PARTICLE THERAPY

The Bragg peak



PROTON THERAPY

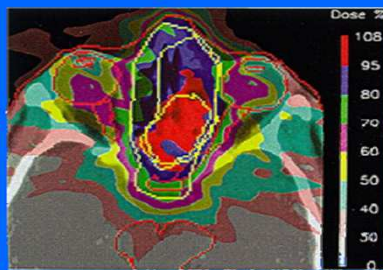


PARTICLE THERAPY

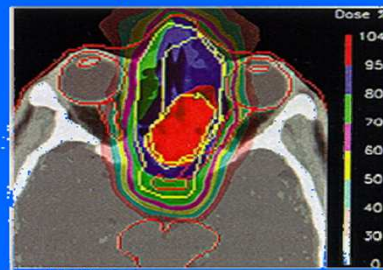
Protons and ions are more precise than X-rays

Tumour between the eyes

9 X ray beams



1 proton beam

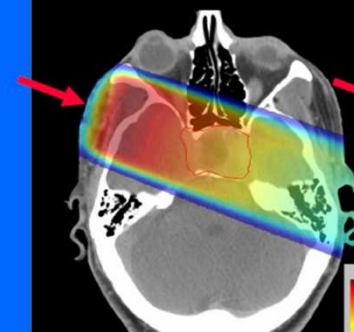


Rome - 14-15.06.07 - SB - 5/5

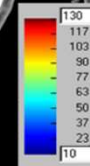
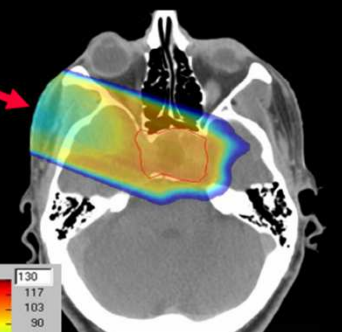
7

Single beam comparison

X rays

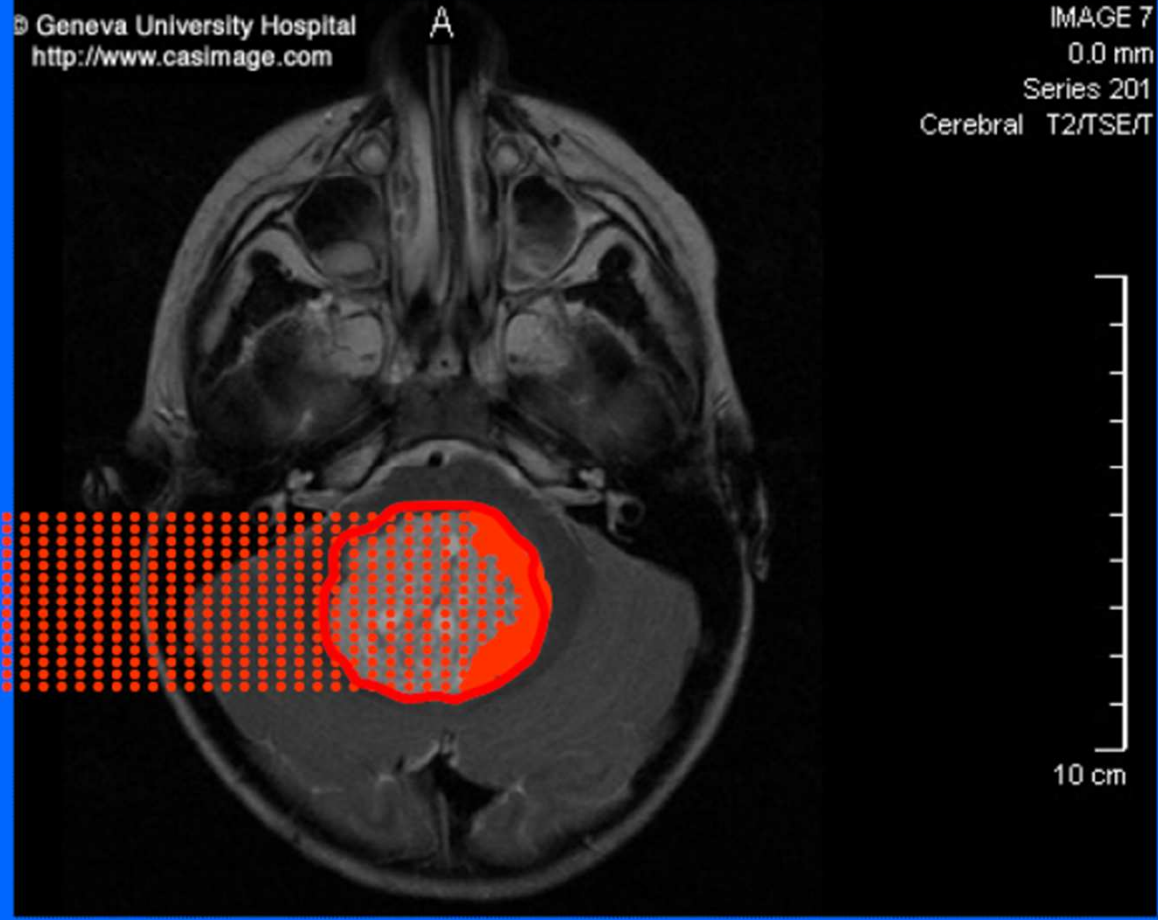


Protons or Carbon ions



Rome - 14-15.06.07 - SB - 5/5

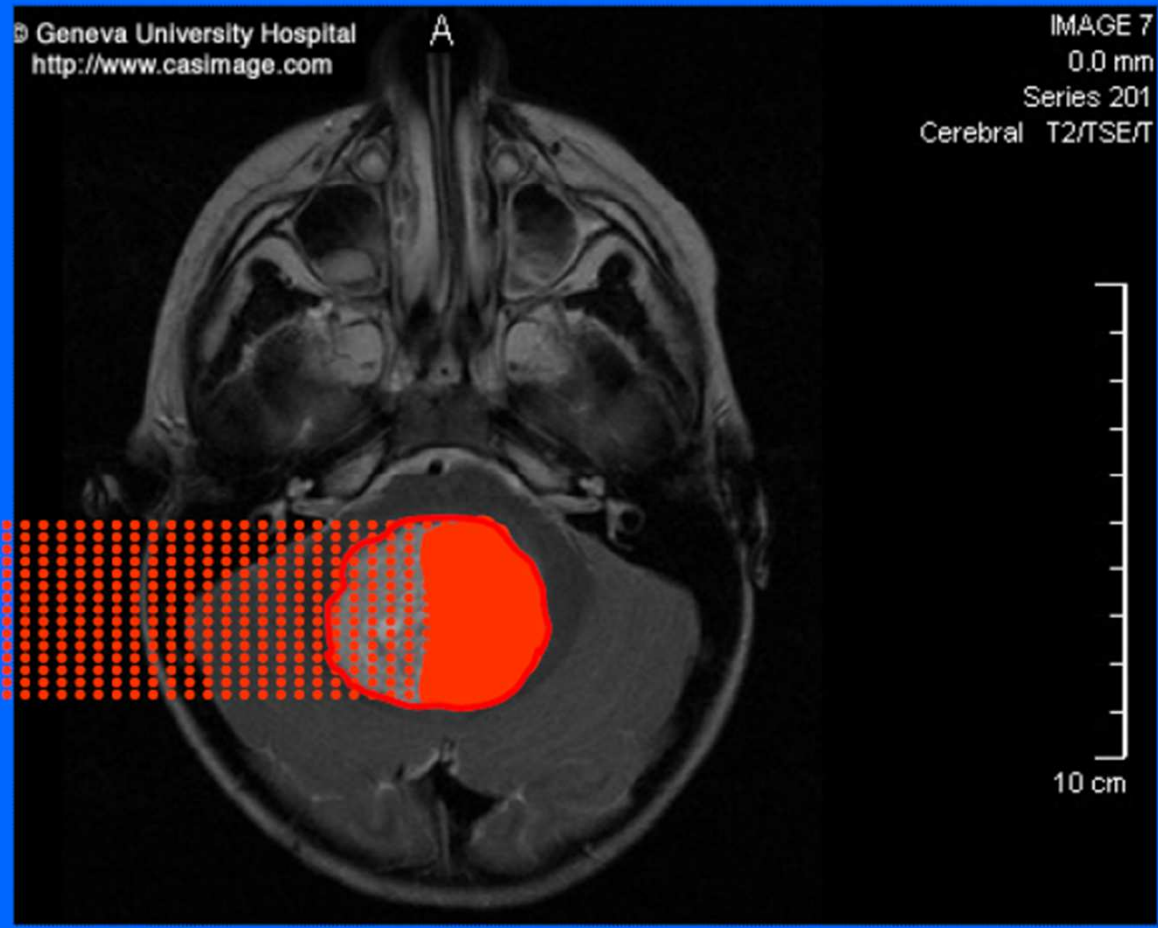
6



High precision RT with proton beams

Rome - 14-15.06.07 - SB - 5/5

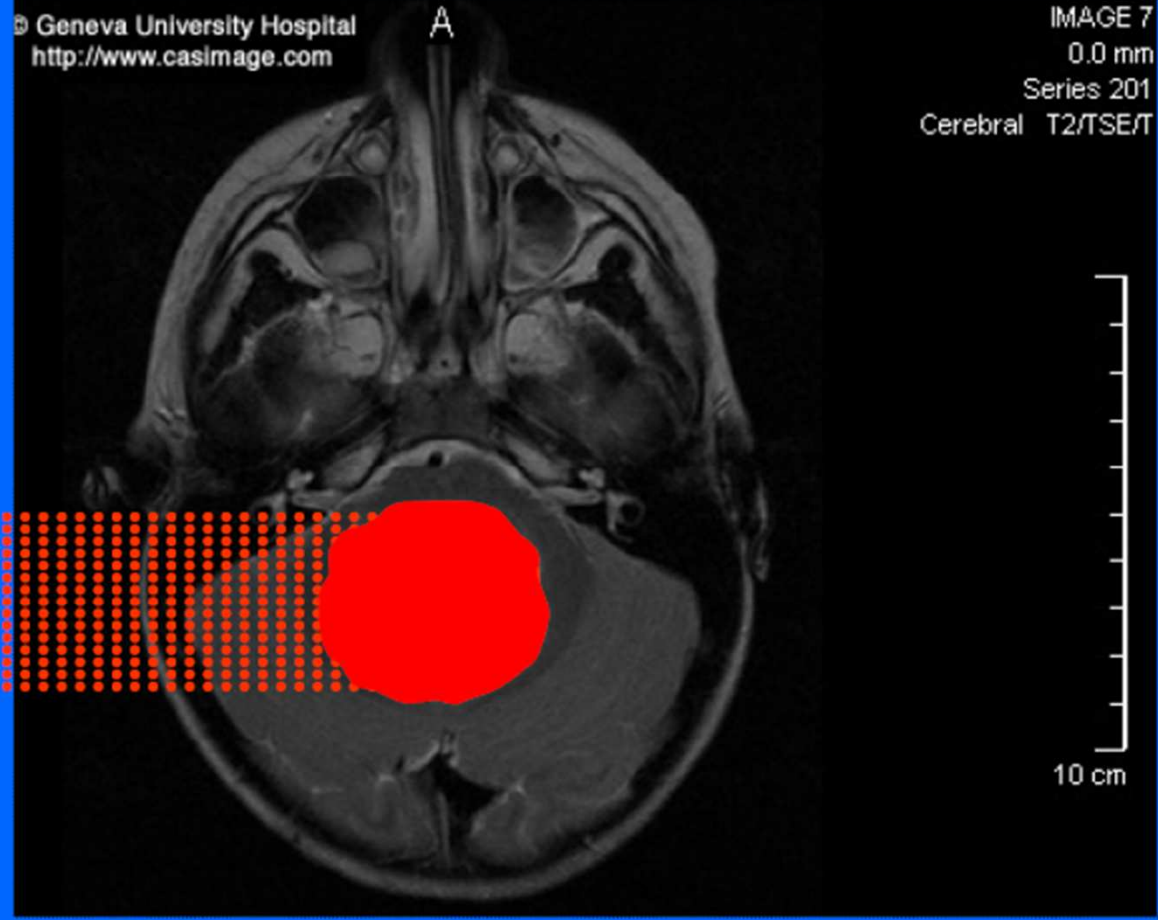
23



High precision RT with proton beams

Rome - 14-15.06.07 - SB - 5/5

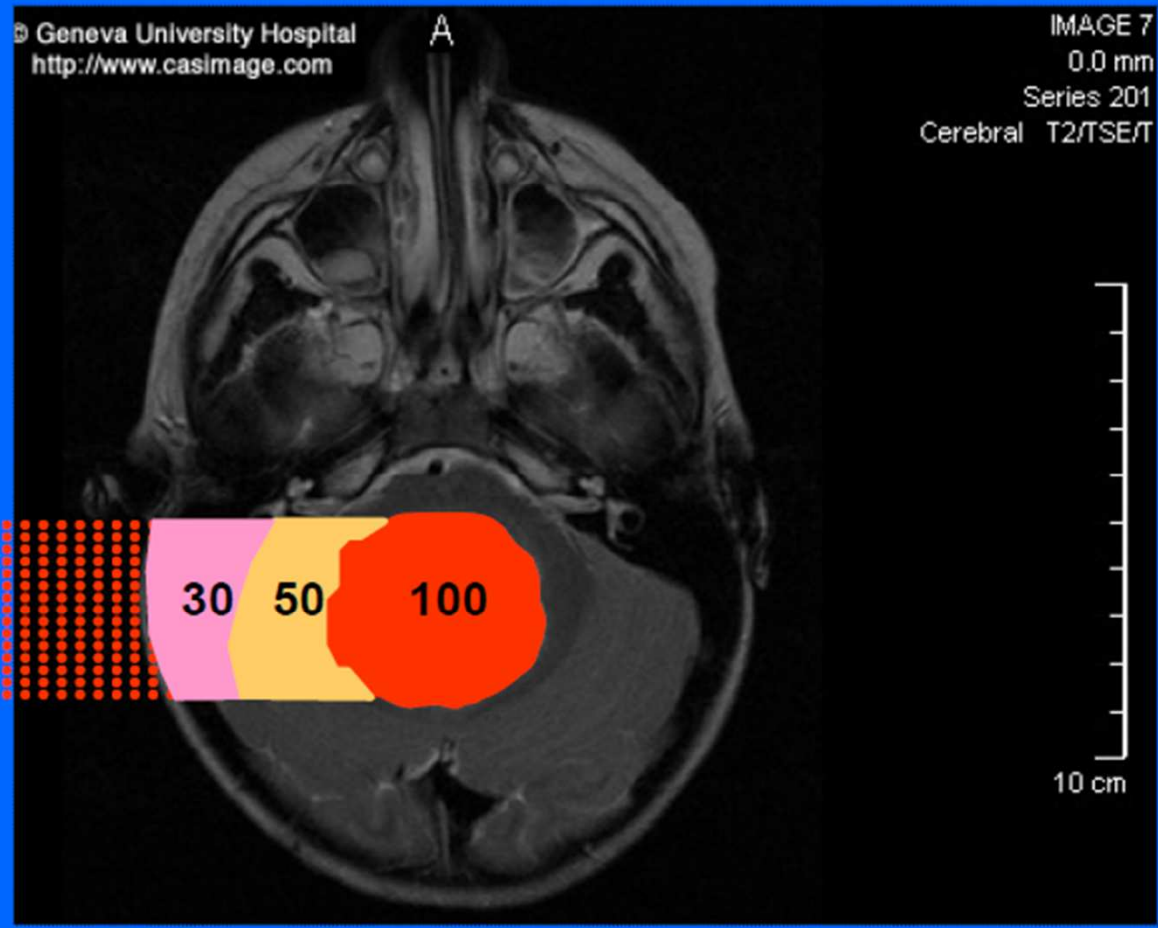
24



High precision RT with proton beams

Rome - 14-15.06.07 - SB - 5/5

25



High precision RT with proton beams

Rome - 14-15.06.07 - SB - 5/5

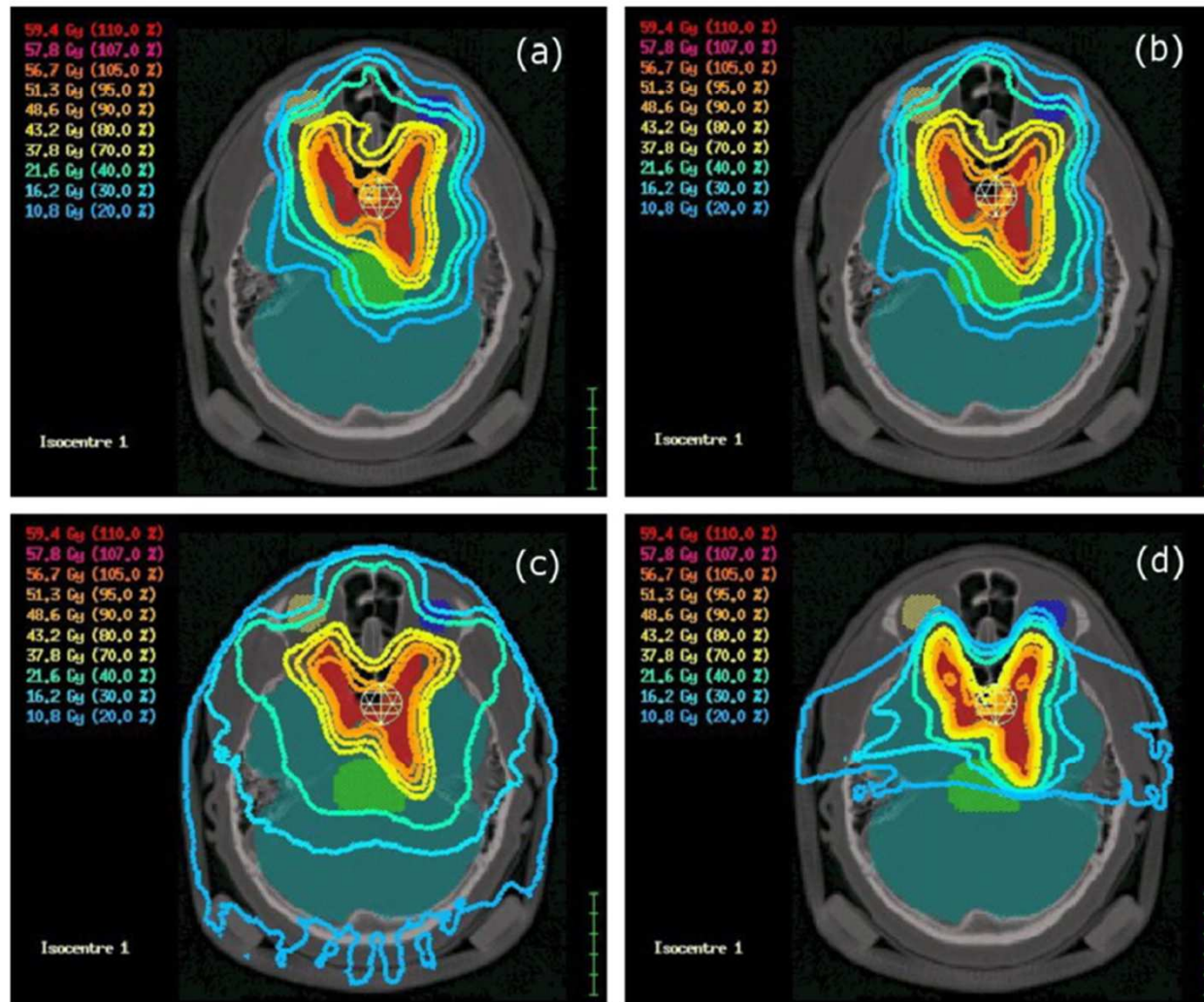
26

Comparison of fixed-beam IMRT, helical tomotherapy, and IMPT for selected cases

Muzik, Soukup, and Alber: Comparison of IMRT, HT, and IMPT

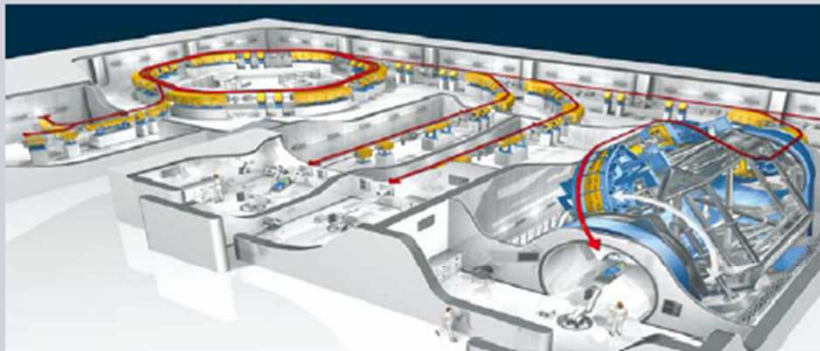
Med. Phys. 35 (4), April 2008

1589



Head-and-neck case B. Comparison of the dose distributions in the isocenter transversal plane. (a) FFM IMRT, (b) sMLC IMRT, (c) HT, (d) IMPT.

PREMIER PROTON THERAPY CENTRES



University of Heidelberg, Germany / GSI and Siemens



NIRS Chiba, Japan / Mitsubishi, Hitachi, Sumitomo



MD Anderson Houston, USA / Hitachi



PSI Villigen, Switzerland / Varian-Accel

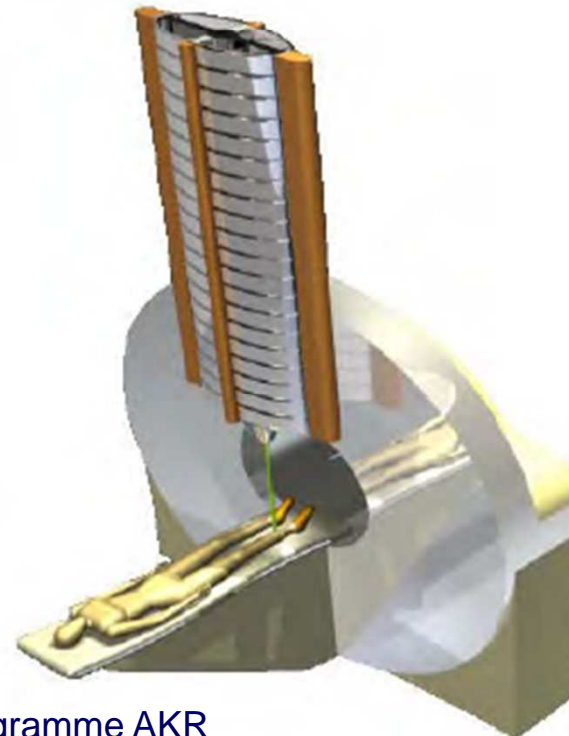


MGH Boston, USA / IBA

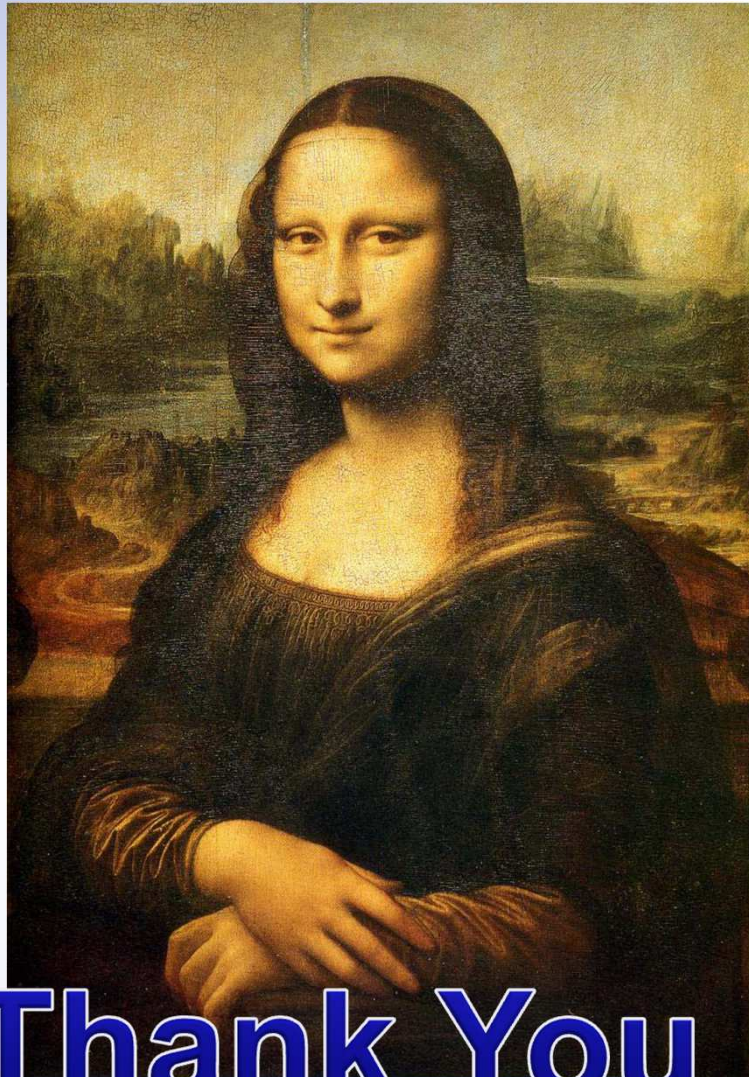


Dielectric Wall Accelerator (DWA)

Compact Particle Acceleration Corporation (CPAC) is developing an IMPT-enabled proton therapy system that will fit into standard, high-energy radiotherapy vaults.



Radiotherapy an art



25 September 2010

Thank You